ELSEVIER

Biochimica et Biophysica Acta 1319 (1997) 19–58

BIOCHIMICA ET BIOPHYSICA ACTA
BBA

Review

Catalytic mechanism of F_1-ATPase

Joachim Weber, Alan E. Senior *

Department of Biochemistry, Box 607, University of Rochester Medical Center, Rochester, NY 14642, USA

Received 2 July 1996; accepted 18 September 1996

Keywords: Oxidative phosphorylation; ATP synthase, F_1F_0-; Catalytic mechanism

Contents

Abbreviations: TF_1, TF_1F_0, the F_1-ATPase, and the F_1F_0-ATP synthase, respectively, from the thermophilic bacterium *Bacillus* PS3; MF_1, MF_1F_0, the F_1-ATPase and F_1F_0-ATP synthase from bovine heart mitochondria; CF_1, CF_1F_0, the F_1-ATPase and F_1F_0-ATP synthase from chloroplasts; AMPPNP, adenyl-5′-yl-imidodiphosphate; TNPATP, 2′,3′-*O*-(2,4,6-trinitrophenyl)adenosine 5′-triphosphate; FSBA, 5′-fluorosulfonylbenzoyl-adenosine; *lin*-benzo-ADP, 8-amino-3-(β-D-ribofuranosyl)imidazo[4,5-*g*]-quinazoline 5′-diphosphate; DCCD, dicyclohexyl-carbodiimide; EIPA, N-ethyl, N-isopropyl-amiloride; NBD-Cl, 7-chloro-4-nitrobenzo-2-oxa-1,3-diazole; NEM, *N*-ethyl-maleimide.

* Corresponding author. Fax: +1 (716) 2712683.

PII S0005-2728(96)00121-1

1. Introduction

ATP synthesis in the membranes of mitochondria, chloroplasts or bacteria is driven by the energy of a proton electrochemical gradient according to the Mitchell mechanism, and is performed by the enzyme ATP synthase. The enzyme consists of two discrete sectors, designated F_0 and F_1, with a stalk connecting the two. F_0 is membrane-embedded, comprised of largely hydrophobic subunits, and provides a pathway for passage of protons through the membrane, down the electrochemical gradient. F_1 is entirely membrane-extrinsic and contains six nucleotide-binding sites, of which three are catalytic sites for ATP synthesis, and three are noncatalytic sites. The enzyme is also commonly called 'F_1F_0-ATP synthase', or 'F_1F_0-ATPase'. The latter name reflects the fact that enzyme from whatever source is reversible in vitro and can act as a proton-pumping ATPase; indeed active extrusion of protons is a physiological function of the enzyme in bacteria under anaerobic conditions, or bacteria that lack proton-pumping respiratory chains. The F_1-sector, when isolated away from F_0, acts exclusively as a net ATP hydrolase. Ease of purification of F_1 has made it a commonly-used experimental model for study of catalytic mechanism.

Research in this area has followed many different paths, for example, into the assembly of this multisubunit membrane enzyme in different cells and organelles, the comparative evolutionary genetics of ATPases, the molecular medicine of human diseases in which the enzyme is defective, and so forth. This review will focus on the enzymatic mechanism of action, with bias toward our own current research focus, namely the catalytic sites. We have concentrated here on reviewing literature published since 1990. Three reviews published at the beginning of the 1990s provided a thorough description of the structure and function of ATP synthase known to that time [1–3]. Several newer reviews have appeared [4–9], and the readers' attention is drawn to two excellent series of short review articles [10,11].

By 1990, a general concept of how the enzyme synthesizes ATP had emerged, which may be briefly summarized as follows. Protons moving down the transmembrane electrochemical gradient through F_0 interact with a specific carboxyl side-chain of subunit *c*, buried in the center of the membrane bilayer. This evokes a protein conformation change in subunit *c*, which is relayed over the distance of more than 80 Å into the catalytic nucleotide-binding sites, via the stalk subunits that connect F_0 to F_1. In one catalytic nucleotide binding site, which is of very high nucleotide-binding affinity, ATP forms reversibly from ADP and P_i ($K_{eq} \sim 1$), due to tight sequestration of products and substrates. The role of the protein conformation change is to drive 'energized release' of ATP, by changing the structure of the high-affinity catalytic site, such that numerous protein-to-ATP interactions, e.g., hydrogen-bonds, hydrophobic interactions and salt-bridges, are broken. The ATP dissociation rate is consequently greatly increased, while ATP binding affinity is decreased, thus allowing net

ATP release into the surrounding milieu [1–3]. An autobiographical sketch by Boyer [11a] summarized the early development of this concept. Kinetic and mutagenesis studies had shown that all three catalytic sites are involved in some way in the overall activity [6,12], and apparent strong cooperativity between catalytic sites was evident in both nucleotide-binding and catalysis [1–3]. However, the exact roles and properties of the three catalytic sites during steady-state activity were not well-established.

Work in the 1990s has been aimed at testing and extending this general concept, refining it quantitatively, and defining it at the molecular level. The following specific areas of study will be given emphasis here. First, knowledge of the structure and function of subunit *c* (the DCCD-reactive proteolipid subunit) has advanced rapidly, mostly through NMR and genetic studies of the *Escherichia coli* protein, together with work on the *Propionigenium modestum* system. Second, the structure and function of the stalk has become clearer. Genetic and protein chemistry studies of the *E. coli* enzyme have revealed critical roles of ϵ and γ subunits, and NMR studies have established the 3D-structure of ϵ subunit. The coupling mechanism can now be said to entail the 'polar loop' of subunit *c*, and the ϵ, γ, δ and *b* subunits, with the *c*-ϵ contact being important at the base of the stalk and the γ-β and ϵ-β contacts important at the stalk-F_1 interface. The ϵ and γ subunits actually play a far more central role in energy coupling than had been previously realized. Third, characterization of the three catalytic nucleotide sites has advanced considerably. Mutations aimed at perturbation of critical catalytic site residues have provided one avenue of information; another important technical approach has been the specific insertion of tryptophan residues to provide direct optical probes of nucleotide-binding during steady-state catalysis. Quantitative aspects of energized release of ATP from the highest affinity catalytic site have also been elucidated.

Last, but emphatically not least, the publication of the X-ray structure of bovine heart mitochondrial F_1 at 2.8 Å resolution [13] has documented a huge amount of new structural information. Virtually all residues of the three α and three β subunits were identified and traced. The architecture of the six F_1 nucleotide binding sites, down to amino acid residue side-chain interactions with nucleotides, was established at the atomic level. While only part of the γ subunit structure was identified, the central role of γ subunit in providing a coupling link between F_0 and F_1 is evident, and contact points, e.g., between γ and β subunits, were determined. At the time of writing the impact of the X-ray structure information is just beginning to show itself in influencing design of experiments, and it may be expected to become a dominant force in the future.

These and other recent advances will each be addressed in detail below. Many significant open questions remain, and indeed we make an attempt to spotlight what we feel are pertinent controversies. The major message will be, however, that a coherent picture of how ATP synthase works at the molecular level is steadily emerging.

2. Structure of F_1F_0-ATP synthase

2.1. Subunit composition

With eight different subunits, the *E. coli* enzyme represents a 'prototype' for ATP synthases. *E. coli* F_1 consists of five different subunits with relative molecular masses of 55 300 (α), 50 300 (β), 31 600

Table 1
Subunit equivalence in F_1F_0-ATP synthase from bacteria, chloroplasts and animal mitochondria

E. coli (Bacteria)	Chloroplasts (Cyanobacteria)	Animal mitochondria
α	α	α
β	β	β
γ	γ	γ
δ	δ	OSCP
ϵ	ϵ	δ
–	–	ϵ
–	–	inhibitor protein
a	*a* (or IV)	*a* (or ATPase-6)
b	*b*, *b*′ (or I,II)	*b*
c	*c* (or III)	*c* (or ATPase-9)
–	–	*d*
–	–	*e*
–	–	*f*
–	–	*g*
–	–	A6L
–	–	F_6

(γ), 19 300 (δ), and 14 900 (ϵ) in a stoichiometry of $\alpha_3\beta_3\gamma\delta\epsilon$; F_0 consists of three subunits with relative molecular masses of 30 300 (*a*), 17 200 (*b*), and 8300 (*c*) in a stoichiometry ab_2c_{9-12} [14]. All eight subunits are required to obtain functional ATP synthase [15,16]. Chloroplast and cyanobacterial ATP synthase has nine different subunits [17] due to the fact that the two *b* subunits are not identical. The animal mitochondrial enzyme has sixteen subunits that have been identified so far [18–21]. Table 1 shows subunit equivalence among bacterial, chloroplast and animal mitochondrial enzymes. Information about yeast and plant mitochondrial ATP synthase subunits may be found in [4,22,23]. The small F_1 subunits δ and ϵ are not analogous in enzymes of different origin: bacterial and chloroplast δ and ϵ correspond to OSCP and δ, respectively, of animal mitochondrial ATP synthase [18,21]. OSCP usually segregates with F_0 in

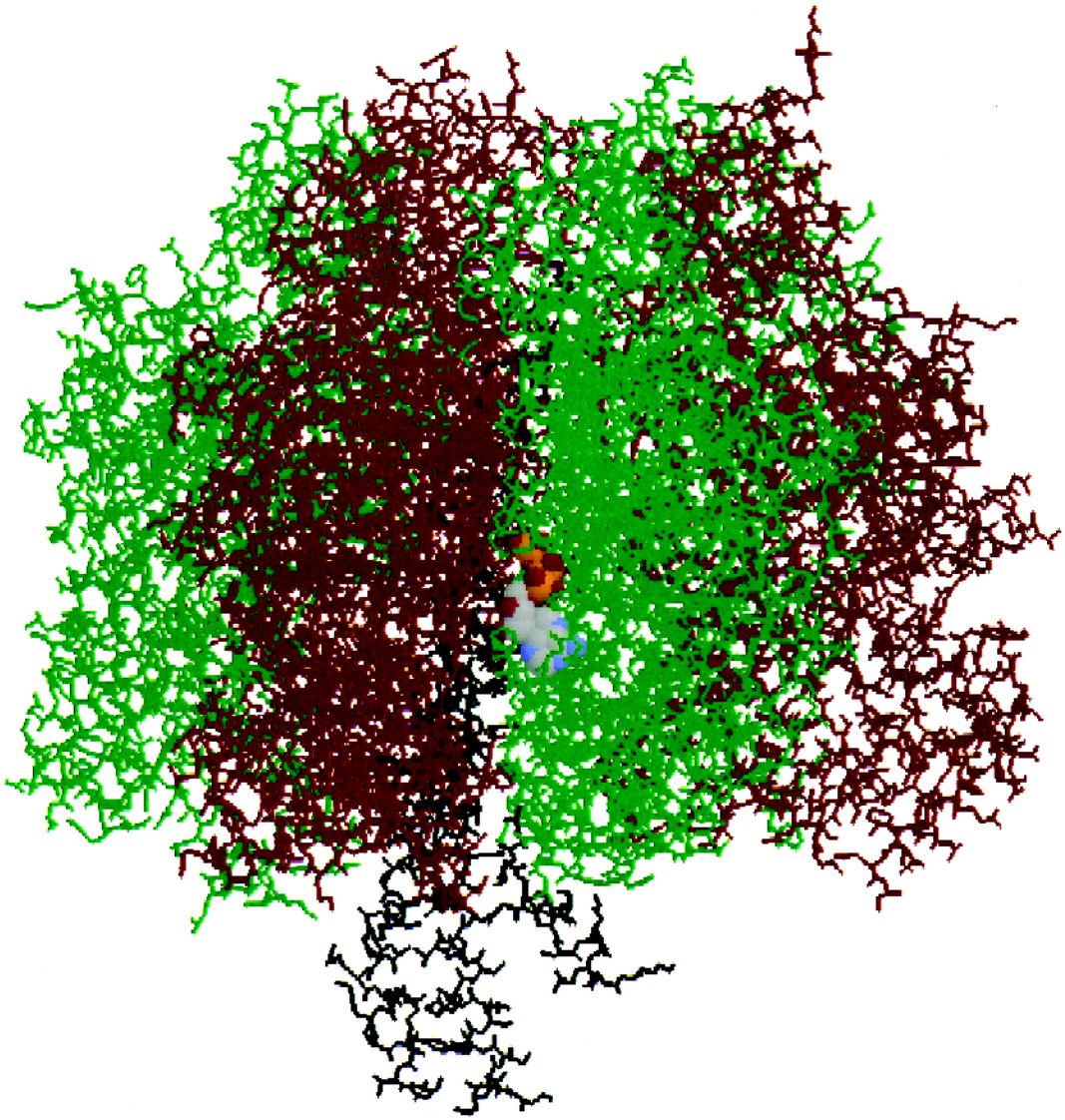

Fig. 1. Structure of F_1 as determined by X-ray crystallography. The structure is from the coordinates determined by Abrahams et al. [13], displayed using the program RasMol (kindly provided by Dr. Roger Sayle, Glaxo Research and Development, Greenford, U.K.). The three β subunits are green, the three α subunits are red, and γ subunit is black. The stalk is at the bottom of the structure. The nucleotide MgATP (actually MgAMPPNP in the crystals) is shown at one catalytic site, in space-filling format. The rest of the structure is shown as a wireframe.

animal and yeast mitochondrial enzyme. Mitochondrial F_1 also contains the 'specific inhibitor protein', not found in bacterial or chloroplast species, whose function is to suppress harmful ATP hydrolysis activity when the proton gradient falls to low levels [24,25]. Further comment will be made on the other 'supernumerary' mitochondrial subunits later.

In *E. coli* the genes for the eight subunits are organized in a single operon, the *unc* operon, which contains a total of nine genes in the order *uncIBEFHAGDC* [14]. The structural genes appear to be arranged in 'building blocks', with *uncBEF* encoding F_0 subunits *a*, *c*, and *b*, and *uncHAGDC* encoding F_1 subunits δ, α, γ, β, and ϵ, respectively. The two large F_1 subunits α and β are very strongly conserved among different species and are homologous also to each other. They probably evolved by duplication of a common ancestral gene (for a discussion of evolutionary relationships among ATP synthases, vacuolar-ATPases and archaebacterial ATPases, see Ref. [26]). The first gene in the operon, *uncI*, encodes a hydrophobic, basic protein which is poorly expressed [27–30], not required to obtain a functional enzyme, and whose role is unknown. Recently it was shown to influence expression or synthesis of subunit *a* [31].

2.2. Structure of F_1

The X-ray crystallography-derived structure of bovine mitochondrial F_1 [13] is shown in Fig. 1. More than 85% of the amino acid residues present in F_1 were identified in the structure, including nearly all of the α and β subunits. However, the small subunits δ and ϵ, as well as about half of the γ subunit residues, could not be located in the electron density map. Consistent with previous electron microscopy studies [8], the X-ray structure shows a six-membered ring of protein masses, representing alternating α and β subunits, surrounding a central cavity containing a mass comprising helical segments of the γ subunit. In contrast to earlier models in which the α and β subunits appeared staggered, similar to the C-atoms in cyclohexane [32,33], the Abrahams et al. structure [13] shows the α and β subunits in the same plane 'like the segments of an orange'. Despite earlier claims based on cross-linking experiments there are no α-α nor β-β subunit contacts.

The α and β subunits both consist of three domains, an N-terminal six-stranded β-barrel (corresponding to *E. coli* residues α19–95, β1–75) [1], a central domain with alternating α-helices and β-strands typical of a nucleotide binding site (α96–382, β76–349), and a C-terminal bundle of six (β350–459) or seven (α383–513) α-helices [13]. The six N-terminal β-barrel domains of α and β are linked to form a crown at the top of F_1 which appears to confer stability on the whole structure. The average distance between adjacent noncatalytic (α) and catalytic (β) nucleotide binding sites is 27 Å (between β-phosphates of bound nucleotide), as had been predicted by fluorescence resonance energy transfer experiments [34]. The distance between two catalytic or two noncatalytic sites is 47 Å; energy transfer measurements in chloroplast F_1 had given values between 36 and 48 Å [35].

Three α-helical sections of the γ subunit were located in the electron density map. The N- and the C-termini of γ are each at the end of a long α-helix, and these two helices are located in the central cavity in the ring formed by the α and β subunits. There are several contact sites between the two helices and the α and β subunits [9,13]. Both helices extend from the base of F_1 about 30 Å beyond the C-terminal domains of α and β, showing that these segments of γ form the top part of the stalk and that in all likelihood the unlocated middle portion of γ is also part of the stalk. Such a location, outside the F_1 sphere was confirmed for a third, rather short, helical portion of γ (γ82–99) resolved in the electron density map. A recent study describes the formation of a cross-link between γ (most likely in the region γ202–230) and a Cys residue introduced into the polar loop region of the *c* subunit, suggesting that γ actually spans the full length of the stalk [36]. This distance, from the membrane surface to the base of F_1, has previously been estimated by electron microscopy to be 45 Å [37,38].

[1] Residue numbering of ATP synthase subunits is different depending on the species. In this paper we use entirely *E. coli* numbering. Residue 'α29' represents α subunit residue 29. Mutations are designated as follows: αG29D represents mutation of residue Gly-29 of α subunit to Asp.

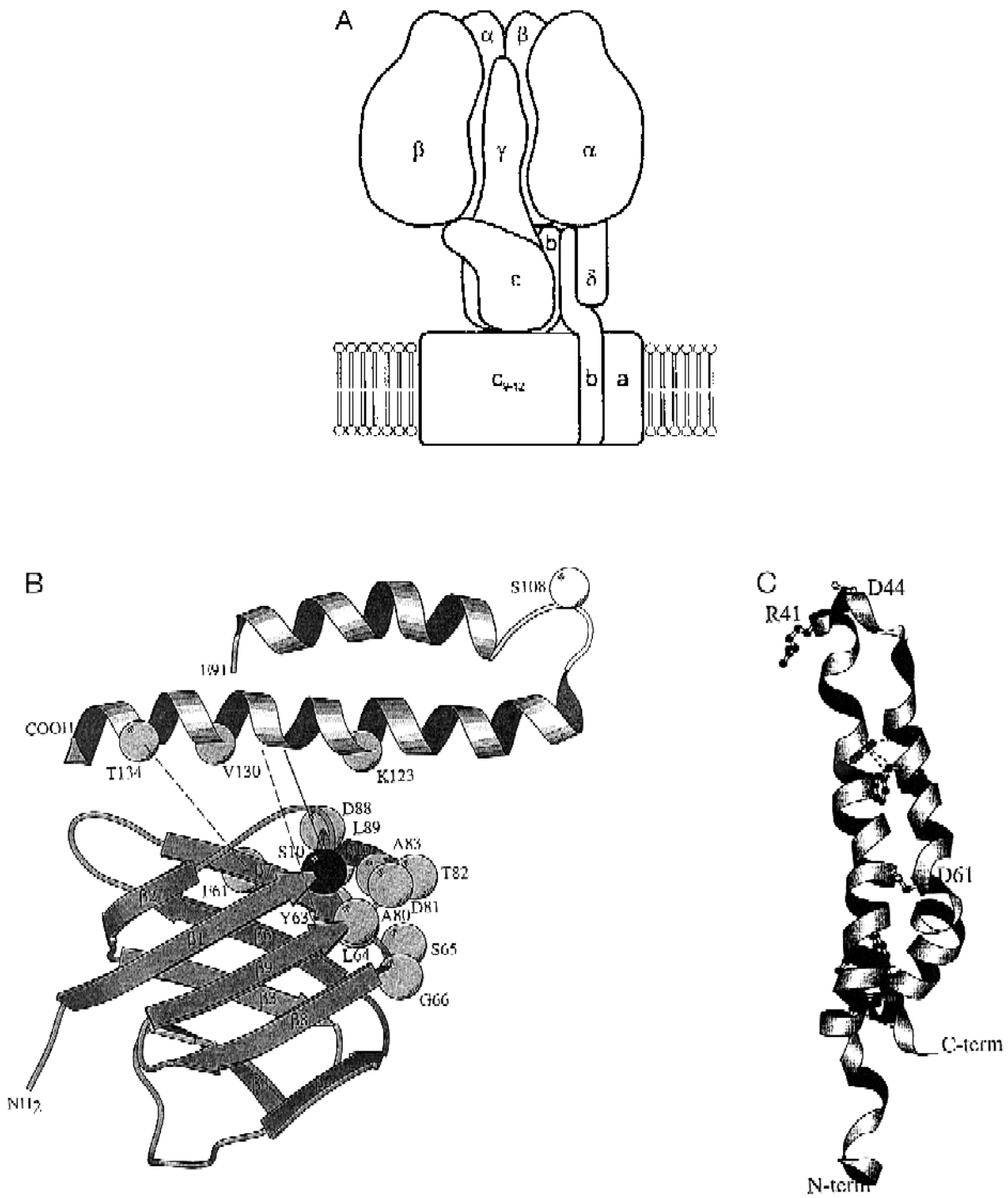

Fig. 2. Structure of entire *E. coli* F_1F_0-ATP synthase and of individual subunits ϵ and *c*. A: F_1F_0-ATP synthase: A tentative diagram of the whole complex. One α and one β subunit, at the front of the $\alpha_3\beta_3$ hexagon, have been omitted. B: Structure of the ϵ subunit: as determined by NMR methods. (Reproduced from Ref. [39] with permission.) C: Structure of the *c* subunit: as determined by NMR methods. (Reproduced with permission from Ref. [121].)

The structure of subunit ϵ of *E. coli* F_1 was solved recently by NMR [39]. It consists of two domains, an N-terminal 10-stranded β-barrel or sandwich (ϵ3–86) and a C-terminal two-helix hairpin (ϵ91–138) (see Fig. 2B). Cross-linking studies indicate that the C-terminal domain is in contact with α and β, and that the N-terminal β-barrel contacts the γ subunit [40–42]. In vitro, binding of isolated ϵ to γ occurs with high affinity (K_d = 3 nM [43]; see also Refs. [44,44a]). Electron microscopic studies indicate that, when looking on F_1 in direction of the rotational (pseudo)symmetry axis through the $\alpha_3\beta_3$ assembly, the ϵ subunit is preferentially associated with one of the β subunits [45]. In addition, there is evidence that the N-terminal domain of ϵ abuts directly on F_0 [46], specifically making contact with the polar loop region of the *c* subunit [47,48]. Taken together this work shows that the ϵ subunit, like γ, spans the full-length of the stalk. Fig. 2A shows the possible arrangement of γ and ϵ in the stalk in F_1F_0-ATP synthase.

The structure and location of δ subunit are not yet established. Isolated δ subunit is known to be elongated and highly helical, and δ is critical for correct binding of F_1 to F_0 (reviewed in Ref. [49]). Based on proteolysis and chemical labelling studies [50], and secondary structure predictions [51], Hazard and Senior [52] proposed a hairpin-like structure for the δ subunit, extending from the center of F_1 through the stalk to F_0. Although subsequent studies, in which a close spatial relationship between the two Cys residues, δ64 and δ140, was shown, indicated that the structure of δ must be more complicated [53], most evidence points to a location of δ in the stalk. Cross-linking, mutagenesis, proteolysis and in vitro assembly studies indicate that δ (or its mitochondrial counterpart, OSCP) makes contact with α and β [15,54–58], and with F_0 subunit *b* [57,59,60].

2.3. Structure of F_0

A low resolution structure of cholate-solubilized F_0 of *E. coli* ATP synthase was obtained by electron spectroscopic imaging [61], which showed subunit *a* and the two copies of subunit *b* located outside of the subunit *c* oligomer. These results were consistent with earlier models [16], based on photolabeling experiments [62] or derived by structure prediction [63]. However, other models place both subunits *a* and *b* within a ring of *c* subunits [64].

Structural information about subunit *a* is limited. It is a very hydrophobic protein, predicted to consist of between 4 and 8 transmembrane helices [65–68]. Direct interaction between subunits *a* and *c* is evidenced by the fact that an *ac* complex that is competent in reconstitution of proton transport can be isolated [69,70]. In a number of the earlier models [1,2,64] one or two predicted C-terminal α-helices of subunit *a* were suggested to make contact with subunit *c*. This is corroborated by mapping of oligomycin-resistance loci, and by analysis of suppressor mutations in subunit *a* which counteract detrimental subunit *c* mutations, as described in Section 3. Evidence for interaction between subunit *a* and *b* comes from cross-linking experiments [71,72] and also from mapping of suppressor mutants [73].

Subunit *b* has a nonpolar segment of about 30 amino acids at the N-terminus, which is predicted to form a transmembrane helix. The remaining 80% of the molecule is hydrophilic, predicted to be highly α-helical and to protrude from the membrane [68,74]. Subunit *b* in F_0 was shown to be dimeric by cross-linking [71,72] and genetic complementation studies [75]. A variety of approaches, including subunit reconstitution, intramembrane photolabelling, cross-linking, limited proteolysis, antibody binding experiments, mutagenesis and revertant analysis showed that the N-terminal transmembrane helix of subunit *b* interacts with subunits *a* and *c* in F_0 and acts as a membrane anchor, whereas the C-terminal hydrophilic extra-membranous segment is required for F_1 binding. These data have been reviewed [1,2,16] and electron spectroscopic imaging studies confirm these ideas [61]. Recently the extramembranous segment of subunit *b* was expressed independently and purified as a soluble dimer [76,77]; it was found to be highly-helical and elongated, as predicted, and it binds to soluble F_1, albeit more weakly than intact *b* does. Electron microscopic studies suggested that the soluble extramembranous *b* fragment interacts with one β subunit in F_1, which is distinct from the β subunit which is associated with ϵ [78]. From a study of mutations occurring in a short hydrophobic sequence of subunit *b*, at residues *b*124 to *b*131, it was concluded that this region provides a helical surface for subunit *b* dimer formation [77].

Subunit *c* is a small, hydrophobic protein, soluble in organic solvents. Analysis of the structure of the *E. coli* protein by NMR techniques has demonstrated that it forms a hairpin consisting of two transmembrane helices connected by a polar loop [79–81], quite similar to what had been predicted from the amino acid sequence [1,2,68]. The NMR data were obtained on isolated protein dissolved in a chloroform-methanol-water mixture; data were presented to show that the protein retains its native shape under these conditions, although it is not oligomeric. The structure model (Fig. 2C) shows two gently curved α-helices, crossing at an angle of 30°, and joined by the polar loop. The C-terminal helix 2 contains at its approximate center the buried DCCD-reactive carboxyl residue (*c*D61) and this helix changes direction by 25° at residue *c*P64 [81]. The ends of both helices appear to be held together by interactions of aromatic residues [81]. Although the detailed structure of the polar loop has not yet been resolved, it is known that this loop points towards F_1 [82,83].

The precise stoichiometry of subunits in the subunit *c* oligomer is not known, and is currently believed to be 9–12 [1,2,65]. It has actually been suggested that this stoichiometry might be variable, depending on the expression of the *uncE* gene [84]. Some models show all the *c* subunits forming a single ring [16,64,85], but other arrangements, e.g., of three units of subunit *c* trimers or tetramers, have also been discussed [16,65].

2.4. Structure of F_1F_0

Based on the foregoing information a tentative diagram of the entire F_1F_0 complex is shown in Fig. 2A. Previous electron microscopy studies showed side views of *E. coli* F_1F_0 with a stalk of dimensions 45 Å in length and 25 Å in diameter, emerging apparently from the central portion of F_0 and joining to the center of F_1 [37,38]. Newer models of F_0 suggest that the stalk may emerge at one side [61]. Interestingly, in cryoelectron microscopic studies of two-dimensionally ordered arrays of chloroplast F_1F_0, Böttcher et al. [86] made the observation that the hexagonal (pseudo)symmetry seen in top views of the F_1 was significantly distorted. This could be due to the fact that the picture is the result of a imposition of the (pseudo)symmetric F_1 on an asymmetric F_0.

The dimensions of the stalk seen in electron micrographs (above) correspond to a protein with a molecular mass of below 20 kDa. As detailed above there are convincing arguments to ascribe over half of the γ subunit as well as all of ϵ to the stalk; this alone results in a protein mass larger than 20 kDa. One proffered explanation [39] is that the averaging procedure used in microscopy leads to elimination of asymmetric elements, such as the ϵ or other subunits. However, it becomes increasingly difficult to include additionally the δ subunit as well as the extramembranous projections of the two copies of subunit *b* in the stalk. Whether there is physical contact between the $\gamma\epsilon$ and the δb_2 subunits remains open, in fact the absence of convincing arguments for such a contact is noteworthy. One can argue that if there is sequential interaction of a specific part of γ or ϵ subunits with each of the three β subunits, in a rotational type of mechanism, as some authors have proposed [64,87], then subunit *b* or δ might be used as a 'stator', connecting the $\alpha_3\beta_3$ assembly with subunit *a*. There is room therefore to speculate that *b* and δ interact with the outside of F_1. At any rate the question as to how, precisely, the F_1 and F_0 are connected is obviously a major remaining structural question.

2.5. The 'supernumerary' subunits of the animal mitochondrial enzyme

The discussion above has been confined to the structure of the 'prototype' *E. coli* enzyme. What is known of the location and structure of the additional eight subunits found to date in the animal mitochondrial enzyme [19,20]? As noted above the specific inhibitor protein is part of F_1, and it interacts with the C-terminal region of the β subunit [88]. The two smallest subunits of F_1, namely δ and ϵ, form a $1/1$ complex in vitro [89,90] and therefore, given that mitochondrial δ is equivalent to *E. coli* ϵ, the mitochondrial $\delta\epsilon$ complex is in the stalk. Also found in the stalk are the subunits F_6 and *d* [18,57,60,90]. Subunit A6L appears to be part of F_0 [18,91] with one part projecting from the membrane at the base of the stalk [57]. The locations of subunits *e*, *f*, and *g* are not yet known. Subunit *f* appears to contain one membrane-spanning helix [19]. Reconstitution of all these subunits into an intact holoenzyme is in progress [60]. Why the animal mitochondrial enzyme should

be so complex in subunit composition as compared to the bacterial is not obvious from functional parameters.

2.6. Summary

The structure of the core catalytic unit of ATP synthase, $\alpha_3\beta_3\gamma$, has been determined by X-ray crystallography, revealing a roughly symmetrical arrangement of alternating α and β subunits around a central cavity in which helical portions of γ are found. A low-resolution structural model of F_0, based on electron spectroscopic imaging, locates subunit *a* and the two copies of subunit *b* outside of a subunit *c* oligomer. The structures of individual subunits ϵ and *c* (largely) have been solved by NMR spectroscopy, but the oligomeric structure of *c* is still unknown. The structures of subunits *a* and δ remain undefined, that of *b* has not yet been defined but biochemical evidence indicates a credible model. Subunits γ, ϵ, *b*, and δ are at the interface between F_1 and F_0; $\gamma\epsilon$ complex forms one element of the stalk, interacting with *c* at the base and α and β at the top. The locations of *b* and δ are less clear. Elucidation of the structure F_0, of the stalk, and of the entire F_1F_0 remains a challenging goal.

3. Energy transduction and transmission in the F_1F_0-ATP synthase

3.1. Overview

Proton movement down the proton electrochemical gradient is the energy-yielding reaction for MgATP synthesis. The subunits of F_0 together provide the proton conduction pathway. It is now generally agreed that protons bind to a critical buried carboxyl group in subunit *c* of F_0 and trigger a conformational change, which is transmitted from F_0 via stalk subunits into the F_1 catalytic sites, where it elicits net MgATP release into the medium [1,2]. Evidence for long-range communication between the buried F_0 carboxyl and the F_1 catalytic sites is strong [92,93]. The older view that transported protons might actually penetrate into the catalytic sites and influence nucleotide chemistry directly has now been discarded. Recent evidence on this point was the demonstration of Na^+-driven MgATP synthesis in F_1F_0 from *P. modestum* and *Acetobacterium woodii* [94–98], and the demonstration that the catalytic site MgATP synthesis reaction equilibrium is unaffected in soluble F_1 by pH [99], or in membrane F_1F_0 by the presence or absence of a proton gradient [100,101]. In MgATP hydrolysis, the reverse process is surmised to occur, with MgATP binding and hydrolysis in catalytic sites bringing about conformational changes in stalk subunits, which are propagated to the buried carboxyl in F_0 and drive proton transport. Occupancy of all three catalytic sites by nucleotide is mandatory for physiological ATP hydrolysis rates [102,103] and probably also for ATP synthesis, although there is no direct evidence yet to prove this latter point.

The buried subunit *c* carboxyl acts as the F_0-energy transducer to trap proton gradient energy in binding energy and use it to convert protein conformation. In *E. coli* this residue is *c*D61 and in *P. modestum* it is *c*E65; both show specific reaction with DCCD, the well-known inhibitor of proton transport, ATP synthesis and ATP hydrolysis. In the 1990s there has been exciting progress in studies of the role of this unique residue. The stalk is the transmission system, relaying conformational signals to the F_1 catalytic sites; progress in understanding the stalk subunits has also been significant. The F_1-located energy-transducer is the trio of catalytic sites, located on the three β subunits. As we discuss later, the three catalytic sites have clearly differentiated affinities for MgATP; in this review we refer to the site of highest affinity as the first site or site one; the site of intermediate affinity is the second site or site two; and the site of lowest affinity is the third site or site three. The first site is proposed to have three essential features: (1) the ability to tightly sequester substrates; (2) as a result of this sequestration, with attendant proximity and stereochemical orientation of substrates in a hydrophobic environment, to catalyse MgATP synthesis from MgADP and P_i with a K_{eq} of ~ 1; and (3) to achieve net energized release of MgATP into the surrounding milieu (e.g., the bacterial cytoplasm or mitochondrial matrix space) on receipt of the appropriate conformational signals from the stalk. Energized release of MgATP, which has been studied directly and in some quantitative detail, will be described in this section, while a more detailed discussion of the characteristics of the catalytic

sites and the reaction mechanism will be discussed in Section 4, following.

3.2. Proton / ATP stoichiometry

A fundamental quantitative property of F_1F_0 is the proton/ATP stoichiometry, i.e., the number of protons transported per ATP synthesized or hydrolysed. It is not known exactly. Recent reports have concluded that the number is 3–4 [104,105]. Accurate knowledge of this number is of importance in calculating the thermodynamic 'balance sheet' of oxidative phosphorylation, and it is also relevant in conceptualizing the mechanism of coupling between F_0 and F_1. For example, if the number is 4, then four subunit *c* molecules may have to first load a proton before one coupled net ATP synthesis event can take place. The stoichiometry of subunit *c* molecules in F_0 is also unknown (Section 2), but the two numbers are hypothetically related as the following example shows. There are three catalytic sites in F_1, thus if four subunit *c* molecules are involved per ATP, a dodecamer of subunit *c* would appear optimal, particularly if one postulates a rotational mechanism; whereas if the proton/ATP stoichiometry is 3, then a subunit *c* nonamer appears more suited. Structural analysis of F_0 and studies of Na^+/ATP stoichiometry in appropriate bacteria should provide answers to these questions.

3.3. Mechanism of proton transport through F_1F_0

In *E. coli*, genetic and purification/reconstitution studies had established that subunits *a*, *b*, and *c*, must all be present for proton transport to occur with physiological characteristics, and there has been for some time persuasive evidence that subunit *c*, and specifically its buried DCCD-reactive carboxyl residue, are directly involved in proton transport, as reviewed previously [1,2]. No other residues of subunit *c*, and no residues of subunit *b*, have been directly implicated in proton transport.

Several subunit *a* residues have been implicated by mutagenesis studies as important for proton transport, as discussed in previous reviews [1,2,4,65] and also in more recent reports [85,106–112]. There is general agreement that residue *a*R210 is essential, that *a*E219 and *a*H245 are significantly sensitive to mutation, and that mutation of several other residues, many of which are found in the C-terminal region after residue *a*190, can have significantly deleterious effects on proton transport and ATP synthesis, depending on the actual substitutions. Proposals have been made which feature some or all of these subunit *a* residues as directly involved in proton transport (e.g., [85,112]) by providing a pathway from the membrane surface to the subunit *c* buried carboxyl, and thence to the opposite side of the membrane. One difficulty is that there is no accepted structural model for subunit *a* (Section 2), and different models place these residues in different locations relative to the bilayer. Some models place residue *a*R210 far from the buried subunit *c* carboxyl [66,113], others place *a*E219 equally removed [67], such that direct interaction between either residue and the buried subunit *c* carboxyl might seem unlikely.

With the finding that Na^+ gradients drive ATP synthesis in certain bacteria, a direct role for subunit *a* residues in proton conduction, by protonation/deprotonation or by providing a continuous 'proton wire' of hydrogen bonds, is eliminated [114]. A more likely scenario is that transmembrane helices of subunits *a* and *c* associate closely to provide an access pathway for protons or Na^+ ions to the subunit *c* carboxyl, perhaps an aqueous pore. Subunits *a* and *c* do associate closely as evidenced by the fact that oligomycin-resistance loci map to both subunits [115,116]. In subunit *a* these mutations fall in the same region as many of those which impair proton transport, i.e., the C-terminal region, and in subunit *c* they map mainly to helix-2. Revertant analysis [66] showed that a combination of mutations in subunit *c* that confers partial impairment of proton transport (*c*A24D,D61G) could be suppressed by mutations in subunit *a* at positions *a*217, *a*221 and *a*224, and also by mutations in helix 2 of subunit *c*. These results support the idea that a specific association between helices of subunits *c* and *a* is necessary to form an ion conduction surface. Thus mutations in subunit *a* that impair proton transport might do so by changing the structural relationship between subunits *c* and *a*.

Whatever the exact role of subunit *a* in proton conduction, there seems to be an assured requirement for subunit *a* to interact with subunit *c* during the catalytic cycle. Taken together with the facts that

subunit *c* is oligomeric as discussed in Section 2, that some subunit *c* mutations are dominant [117] and impair proton transport when present in the proportion of one copy per oligomer [118], and that DCCD blocks proton transport at a stoichiometry of one reacted subunit *c* per F_1F_0 [119], this provides inferential evidence for movement of the single copy subunit *a* from one subunit *c* molecule to another during catalysis, as was envisaged, e.g., by Cox and colleages [64,120] in their 'rotational catalysis' mechanism in which subunit *a* rotates within an oligomeric ring of subunit *c*, or by Vik and Antonio [85] who suggested that subunit *a* rotates around the periphery of the subunit *c* oligomer.

3.4. The critical role of the buried carboxyl of subunit c in proton transport and energy transduction

3.4.1. Proton transport

As described above in Section 2, NMR structural analysis of purified *E. coli* subunit *c* has revealed that it is a helical hairpin with a polar loop connecting the two helices (see Fig. 2C). The polar loop extends from the cytoplasmic F_1 side of the membrane, the buried carboxyl cD61 lies in the center of the membrane in the C-terminal helix-2 [121]. The micro-environment of the carboxyl group has been studied in terms of its relation to surrounding residues, and it is seen that it lies in a hydrophobic environment, where there is local unfolding of helix-2 [80,81,122,123]. A mutant in which the carboxyl is moved to the apposing helix-1 (*c*A24D/D61G) is partly functional [123], and its *c*D24 carboxyl appears to be located in the same position as the *c*D61 carboxyl in wild-type [81]. Residues *c*A24 and *c*D61 make Van der Waals contact in wild-type. A series of other partly-functional mutants with various buried carboxyl residues has been obtained [124], and the conclusion, that a buried carboxyl in the specific environment that normally surrounds *c*D61 is critical for proton transport and energy coupling function, is strongly-supported.

pK_a values of the carboxyl side-chains in wild-type *E. coli* subunit *c* were analysed by NMR, and it was seen that the *c*D61 carboxyl, alone of the six carboxyl residues in subunit *c*, had significantly elevated pK_a, of 7.1 [125]. Furthermore, the mutant *c*D24 carboxyl also showed similar elevation of pK_a, to 6.9. This is consistent with previous proposals, that the pK_a of this residue should be elevated in at least one step of the catalytic cycle [1,2], and that protonation/deprotonation of this residue is involved directly in proton transport. Thus, in ATP synthesis protons would bind from the outer side to the low pK_a form, and be released to the inner side from the high pK_a form.

Insights into subunit *c* function have come from an unanticipated quarter, the study of the organism *P. modestum* which drives MgATP synthesis by F_1F_0 using an Na^+-gradient. Dimroth and colleagues showed that the F_1F_0 of this organism is similar to that of other bacteria in architecture, and the amino acid sequence of subunit *c* resembles that of counterparts in *E. coli*, other bacteria, mitochondria, and chloroplasts [95,114]. The buried carboxyl residue of subunit *c* in *P. modestum* F_1F_0 (*c*E65) reacts specifically with DCCD, and reaction blocks ATP hydrolysis by F_1 [126,127]. Na^+ or Li^+ protected against DCCD-reaction with residue *c*E65, and protection, like DCCD-reaction, was strongly pH-sensitive. The authors conclude that the *c*E65 carboxyl provides a specific Na^+-binding site, at which Li^+ and protons compete with Na^+ for binding, that the protonated carboxyl reacts with DCCD, and the unprotonated carboxyl binds the ion. The data indicated that the pK_a of *c*E65 is ~ 7, and Na^+ binding appeared to promote deprotonation. From the pH-sensitivity of the DCCD-reaction and the protection by Na^+, the authors propose a chemical reaction scheme for DCCD-inactivation and suggest that stimulation of the ATPase activity of F_1F_0 by Na^+ involves three interacting ion binding sites [127]. Subsequent work on purified subunit *c* confirmed that the *c*E65 carboxyl is the site of ion binding [128]. Work on isolated F_0 from *P. modestum*, reconstituted in proteoliposomes, showed that it transported ions by a carrier-type mechanism, confirming the presence of an Na^+ (or proton) binding site, and demonstrating ability of the unliganded binding site to re-orient its apparent membrane sidedness in a membrane-potential-dependent step [129]. In the view of these authors the hydronium ion, not the proton, is the ion which competes with Na^+ for binding to *c*E65, and is the true counterpart of the Na^+ ion in 'protonophoric' species such as *E. coli*. They suggest [127] that the unprotonated buried carboxylate of subunit *c* binds

the ion from one side of the membrane, a conformational change reorients the carboxylate-ion complex, and then an Arg side-chain displaces the transported ion by forming a salt-bridge with the carboxyl (see below), and the ion leaves at the opposite side of the membrane. In this mechanism, changes in the pK_a of the carboxyl during the catalytic cycle are not required.

It is evident that the immediate environment around the buried carboxyl group is critical for ion specificity of ATP synthesis in different species. For example, substitution of the string of four residues *c*60 to *c*63 in *E. coli* subunit *c* by the analogous string of residues from *P. modestum* subunit *c* converted *E. coli* F_1F_0 into an Li^+-sensitive ATPase, reminiscent of the *P. modestum* enzyme, although it did not appear to confer Na^+-sensitivity [130]. Conversely, mutations in residues in helix-2 of *P. modestum* subunit *c* caused loss of Na^+ binding but retention of Li^+ and proton binding [131].

Amiloride is a well-known inhibitor of mammalian Na^+- transporters. A hydrophobic analog (EIPA) was found to inhibit ATPase activity of F_1F_0 of *P. modestum* and to competitively protect subunit *c* from DCCD reaction [127,128]. Several hydrophobic analogs of amiloride also inhibited the ATPase activity of *A. woodii* F_1F_0 [96] and were shown to compete with Na^+ and DCCD for a common binding site in subunit *c* [132]. Amiloride and derivatives are guanidinium compounds, and it was proposed that they bind to the unprotonated subunit *c* buried carboxyl to build a salt-bridge [127]. The protonated guanidinium could also resemble a protonated, reactive DCCD species. This led to the hypothesis [127] that both amiloride derivatives and the reactive DCCD species might be mimicking an Arg side-chain which normally interacts with the buried carboxyl at one step of the transport process, as was described above. Possible candidates are *a*R210 of subunit *a*, mentioned above, and the conserved *c*R41 of the polar loop of subunit *c*. Fraga et al. [66] have also considered the possibility of direct interaction of an Arg side-chain with the *c*D61 carboxyl; in their view the role would be to lower the pK_a of the carboxyl at one step of the transport cycle.

F_0 acts as a passive ion carrier when F_1 has been stripped away, and isolated F_0 has been used extensively in studies of structure and function of the proton transport pathway. Fillingame et al. have recently argued that the proton conduction mechanism in isolated F_0 need not exactly correspond to the active process in F_1F_0, and have discussed genetic evidence to support this view [121]. A high pK_a form of the buried carboxyl is likely to be the form that mediates passive proton translocation by F_0 [125,129].

3.4.2. Conformational changes in subunit c triggered by ion binding to the buried carboxyl

Interaction of protons with the buried subunit *c* carboxyl was proposed to trigger conformational changes within the subunit *c* molecule which alter conformation of the polar loop [1,2]. Genetic evidence for this idea comes from mutations in conserved residues of the polar loop, at *c*R41, *c*Q42, and *c*P43, which produce an uncoupled phenotype in which proton transport per se is functional, but correct integration between F_0 and F_1 is interrupted, hence ATP synthesis and ATP-driven proton transport are defective, ATPase activity is DCCD-insensitive, and F_1 binding to F_0 does not block passive proton transport as it normally does in wild-type [133–137]. New evidence that proton interaction with the buried carboxyl triggers a conformational change in the polar loop has now come from NMR experiments. Reaction of *c*D61 with DCCD was seen to bring about conformational changes at *c*D44 [79]. Titration of the cD61 carboxyl was seen to alter the conformation of the region from *c*A39 to *c*P43 upon deprotonation of the *c*D61 carboxyl [125]. It seems very likely that these conformational changes are manifestations of the coupling mechanism.

3.5. The interface between F_0 and the stalk

Subunit *b* has been established as a component of both F_0 and stalk (Section 2). At the present time the evidence strongly supports a structural role for subunit *b* in binding F_1 to F_0; however, there is no indication yet of a dynamic role in the coupling process. Similarly, as reviewed above (Section 2), subunit δ, and its mitochondrial homolog OSCP, is also involved in binding F_1 to F_0. In chloroplasts and mitochondria direct binding of this subunit to F_0 is seen, whereas in bacterial species, and also chloroplasts, the subunit purifies with F_1. Thus subunit δ is

apparently present at both F_0-stalk and stalk-F_1 interfaces. Cross-linking and proteolysis studies indicated that the N- and C-terminal regions of δ interact with F_1, leaving a large central part of the subunit as candidate for interaction with F_0 [50].

Recent work showed that subunit *c*-ϵ interaction occurs at the F_0-stalk interface, and appears to be of considerable importance in energy coupling. The first evidence came from revertant analysis in which mutations in ϵ were shown to suppress the mutation *c*Q42E in the polar loop of subunit *c* which gave uncoupled phenotype [47]. All of the suppressor mutations were found at residue ϵ31, and they corrected the coupling defect. In follow-up studies [48], Cys residues were inserted in the polar loop of subunit *c* at positions surrounding the parent mutation and also at position 31 in ϵ. Disulfide cross-links were obtained in high yield between residue ϵ31 and residues *c*40, *c*42, or *c*43, clearly demonstrating close physical proximity of the polar loop of subunit *c* and ϵ subunit. The cross-linked enzymes were inhibited in respect to ATP-driven proton transport. This evidence strongly supports the statement that subunit *c*-ϵ interaction is a critical feature of conformational coupling at the F_0-stalk interface. In similar experiments, cross-linking between γ and *c* subunits was also obtained, albeit in low yield, implying that γ subunit may also interact with subunit *c* [36]. However, no functional consequences can yet be attributed to this finding.

3.6. The stalk-F_1 interface

As noted above, the C-terminal region of δ subunit is known to interact with F_1, and recent work has emphasized that it is functionally important in energy coupling. Deletions from the C-terminus of both mitochondrial OSCP and *E. coli* δ impaired F_1 binding and coupling [138,139]. In a systematic study involving first random mutagenesis and then localized and site-directed mutagenesis, it was seen that the C-terminal region was most susceptible to functional impairment. Two residues of particular importance were δA149 and δG150, and a series of mutants at these two positions could be categorized in terms of relative degree of impairment of energy coupling [52,140]. This region appears to lie close to the α subunit of F_1, since disulfide cross-links were seen between residue δCys-140 and α subunit [50].

Recent work has demonstrated conclusively that ϵ subunit makes contact with α [141] and β [41,42,46,142] subunits of F_1. The contacts occur between the helical region of ϵ subunit and the C-terminal domains of the α and β subunits, and have been established in considerable molecular detail in cross-linking experiments, often in combination with specific insertion of Cys residues by mutagenesis. Moreover, both cross-linking experiments and electron-microscopy [143] have indicated that the specific ϵ-α and ϵ-β interactions appear to be dependent on and changed by nucleotide occupancy of the catalytic sites, leading to the proposal that ϵ subunit moves between α and β subunits during catalytic turnover and the hypothesis that this movement is related to coupling between F_1 and F_0 [144].

Functional involvement of the γ subunit in energy coupling was shown by the isolation of mutants in γ which cause uncoupling of ATP synthesis or hydrolysis from proton transport [145]. Second-site suppressor mutations were obtained in regions of the γ subunit which do not interact directly with the parent mutations [146,147]. Rather they are at positions in three helical regions of γ which affect interactions between γ and β subunits [9]. In a further set of mutagenesis experiments, a frame-shift mutation in γ subunit causing a C-terminal extension of 16 amino acids was shown to be suppressed by mutations in the β subunit [148]. Thus genetic evidence for functional involvement of γ-β subunit interaction at the stalk-F_1 interface is compelling.

There is extensive and detailed evidence from cross-linking experiments for specific γ-β subunit interactions [42,87,142,149–151]. Cross-links could be obtained between γ and the C-terminal domain of β, and also intriguingly between residue γ8 and β subunit residue 148, which is very close to the conserved ‘P-loop’ sequence that binds the phosphate end of MgATP in the catalytic sites [151]. Several of the cross-links were observed to be dependent on and changed by nucleotide occupancy of the catalytic sites (refs. cited), implying that nucleotide binding induces movements of γ subunit relative to β, and this is supported by electron microscopy [45]. On the basis of nucleotide-induced cross-linking experiments between β and γ, it has recently been hypothesized

that the γ subunit actually rotates in relation to the β subunits during turnover [87]. Cross-linking of β and γ inhibits enzyme turnover.

Fluorescent labels attached to the γ subunit at specific residues (γ8 and γ106) show enhancement of fluorescence when nucleoside triphosphate (MgATP or MgAMPPNP) is bound in the first catalytic site, but not when MgADP is bound [152,153]. With MgATP, the fluorescence enhancement was transient and decayed with hydrolysis. This evidence shows that in addition to inducing translocations of the γ subunit, nucleotide-binding in the first catalytic site induces conformational changes in γ subunit in a specific fashion. If proton transport-induced signals can cross the same conformationally-sensitive γ-β interface in the opposite direction, then this could be a pathway of signal transmission into the catalytic site.

Subunits ϵ and γ are known to form a tight complex [43,44,44a] and details of the contact points between them in F_1 have been established [154,155]. It appears that the ϵ-γ contact points occur in a domain of γ that is not defined by the X-ray structure, i.e., lower down in the stalk. Thus these two subunits are almost certainly acting in concert in the stalk. Capaldi and colleagues [42,142] have proposed that each of the three β subunits may be distinguished, depending upon its interaction with ϵ and/or γ. Thus one β interacts with γ, the second with ϵ, and the third with neither ('β-free'). Binding of nucleotide to each of the β subunits was studied by photoaffinity labelling and it was seen that the first catalytic site resided on the 'β-free' subunit, the second site on the 'β-ϵ' subunit, and the third site on the 'β-γ' subunit [156]. Thus, translocation of the γ and ϵ subunits between β subunits is likely to correlate with re-orientation of the first, second and third catalytic sites among the three β subunits. Such switching of the catalytic sites is thought to be an integral feature of catalysis, as discussed in Section 4.

Summarizing this section, this has been an active area of investigation. What has become apparent is that the γ and ϵ subunits play major roles in coupling between F_0 and F_1, that they are both found in the stalk and interact together closely, that they contact subunit *c* in F_0 and both α and β subunits in F_1, and that they move in relation to the α and β subunits in response to binding of different nucleotides. The three β subunits may be distinguished in terms of their interaction with γ and ϵ. It may be hypothesized that movement of γ and ϵ relative to α and β is required and integral to catalytic turnover. So far, however, none of these movements has been shown to be generated by a proton gradient, nor to be correlated with either ATP synthesis or ATP-driven proton transport.

It has been hypothesized by many groups that there may be rotation of the minor subunits γ and ϵ within the $\alpha_3\beta_3$ hexagon during catalysis. This intriguing idea is thought to be consistent with the X-ray structure [13] and could also be considered consistent with electron microscopy studies [45]. It has been strongly-promoted recently on the basis of cross-linking studies [87]. We would add a cautionary note, that it is important to distinguish true rotation from just subunit movement. Proof of rotation would appear, at minimum, to require demonstration of movement of subunit γ (or another subunit) in strict sequence, from $\beta 1 \rightarrow \beta 2 \rightarrow \beta 3 \rightarrow \beta 1$.

3.7. Energized release of MgATP from catalytic sites

Direct evidence that a proton gradient derived from respiratory chain substrate oxidation could drive release of ATP from an F_1F_0 catalytic site was first derived by Penefsky [157] in mitochondrial membrane particles. The experiment was to bind [γ-^{32}P]MgATP in substoichiometric amounts to the first catalytic site, to initiate oxidation of NADH or succinate, and to trap the released ATP with hexokinase/glucose. In more recent work, the experiment has been repeated in *E. coli* membranes [158], and a quantitative analysis of the phenomenon has been carried out in mitochondrial membranes [159,160]. This demonstrated that a proton gradient changes the dissociation rate for ATP from the first, highest affinity, catalytic site by more than six orders of magnitude, while leaving the association rate largely unaffected. Thus the apparent binding affinity (K_d) for MgATP at site one is considerably weakened, by around seven orders of magnitude. Calculations showed that K_d for MgATP in the presence of an induced proton gradient and 0.1 mM MgADP could approach 10^{-3} M. ATP was released at a rate fast enough to be consistent with ATP synthesis rates by oxidative phosphorylation.

In vivo, there must be net release of ATP into the medium, which in the case of *E. coli*, for example, is the cytoplasmic compartment containing approx. 3 mM ATP, 0.4 mM ADP (or lower), and 6 mM P_i [161]. It is not, in fact, sufficient that the proton gradient should generate a conformational change in the first catalytic site that increases the off-rate for MgATP and decreases its affinity. In order to achieve net ATP synthesis, rebinding of ATP from cytoplasm must be prevented (Fig. 3, top), i.e., ADP must compete successfully with ATP for binding at one or more catalytic sites, even though it is present in at least 10-fold lower concentration in the surrounding milieu. Given that there are more potential ligand-binding determinants on an ATP molecule as compared to an ADP molecule, this would seem to be an interesting challenge for the enzyme.

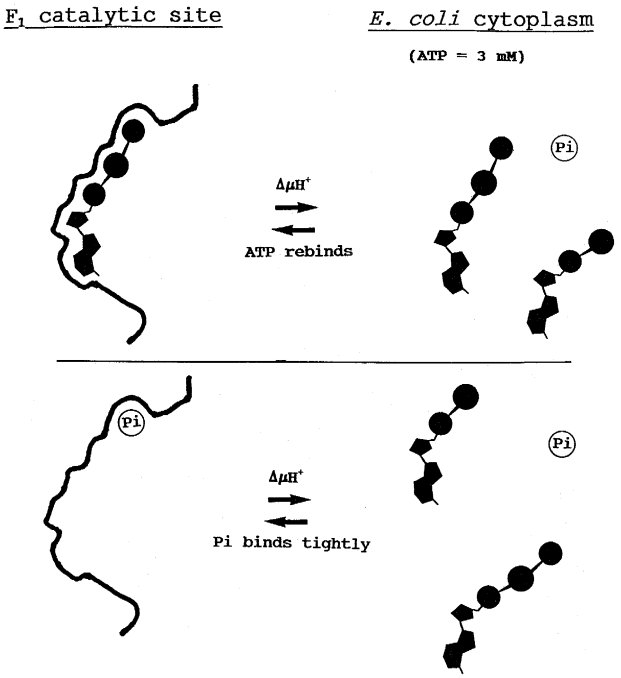

Fig. 3. Energized release of ATP from F_1 induced by the proton gradient. The top part of the figure shows the release of ATP induced by the proton gradient ($\Delta\mu H^+$) into the *E. coli* cytoplasm, where ATP concentration is $\sim$3 mM, i.e., about 10-fold the ADP concentration. As discussed in the text, unless there are mechanisms to prevent ATP from rebinding, net ATP formation will not occur. The bottom part of the figure shows a suggested solution to the problem. The proton gradient greatly increases P_i binding affinity. P_i bound in the catalytic site then blocks ATP rebinding, and allows only ADP binding.

P_i does not bind to soluble F_1 catalytic sites ($K_d(P_i) > 10$ mM [102,162]). Thermodynamic analyses of the catalytic pathway in *E. coli* enzyme showed that even at the first catalytic site the $K_d(P_i)$ was > 1 M [99,163], and provided strong evidence that P_i binding affinity must be greatly enhanced in the presence of the proton gradient [163]. This has now been confirmed by the finding that $K_m(P_i)$ during ATP synthesis by reconstituted *E. coli* F_1F_0 in the presence of a proton gradient is 0.7 mM [164]. Energized binding of P_i could effectively block rebinding of ATP and favour binding of ADP, because P_i would occupy the γ-phosphate position of the nucleotide site (Fig. 3, bottom). In contrast, binding affinity for MgADP is unaffected by the proton gradient. In soluble F_1, the catalytic sites of lowest affinity showed K_d(MgADP) of 20 μM in the absence of P_i and 29 μM in the presence of 5 mM P_i [102]. The K_m(MgADP) for ATP synthesis in the presence of a proton gradient was 27 μM [64]. Therefore during oxidative phosphorylation there is energized binding of P_i but not of MgADP, and we suggest it is the energized binding of P_i that blocks ATP rebinding, as in Fig. 3, bottom.

The experiments on energized release of ATP from the first catalytic site of F_1F_0 in mitochondrial and *E. coli* membranes, described above, were performed in the presence of a hexokinase/glucose trap, thus the ambient ATP concentration in the medium was zero. It is of importance, therefore, to establish an experimental system in which nucleotide occupancy and affinity of all three catalytic sites can be directly monitored during ATP synthesis, and net energized release of ATP can be followed, under conditions of ambient nucleotides mimicking those in vivo.

3.8. Summary

Respiration-induced proton gradients do induce conformational changes in the first high affinity catalytic site which greatly increase K_d(ATP) and could in principle lead to net energized release of ATP. The preceding arguments suggest that the sequence of events is: (1) binding of the ion (proton, hydronium, or sodium) to the buried subunit *c* carboxyl, which triggers (2) a binding energy-induced change of the conformation around the buried carboxyl, which is

(3) transmitted through subunit *c* to the polar loop region, where it (4) crosses the *c*-ϵ and perhaps the *c*-γ subunit interfaces, promoting (5) wholesale relocation of the stalk subunits, particularly ϵ and γ, probably also the C-terminus of δ, resulting in (6) translocation of ϵ and γ relative to β and α subunits, and ultimately (7) change of conformation of catalytic site one, with resultant reduced affinity for ATP.

Future profitable directions seem clear. It is important to obtain the full structures of subunits *a, b* and δ, and to complete those of *c* and γ. While cross-linking procedures have proven useful so far in revealing subunit interfacial contacts and apparent movements of subunits, this approach does have limitations. Thus development of alternative procedures to evaluate subunit movements will be imperative. Intra-subunit conformational changes are clearly of major importance, particularly in the β subunits which carry the catalytic nucleotide-binding domains, and techniques to follow them in real time must be developed. Similarly, probes must be developed to allow direct monitoring of occupancy and affinity of all three catalytic sites during ATP synthesis in the presence of nucleotide and P_i concentrations in the medium similar to those occurring under physiological conditions.

4. Catalytic sites: structure, function, mechanism

4.1. The catalytic subcomplex: F_1

The ability to obtain isolated F_1 in high yield and purity has in the past made this soluble subcomplex the system of choice for investigation of catalytic mechanism. Isolated F_1 is able to catalyze ATP hydrolysis but not net ATP synthesis. For the study of many aspects of the mechanism this activity is sufficient. With the mitochondrial enzyme it was demonstrated that accessible catalytic rate and equilibrium constants are virtually the same for isolated F_1 and membrane-bound F_1F_0 [165]. In the case of *E. coli* enzyme, it was shown that catalysis-related movement of γ subunit relative to the three β subunits seen in isolated F_1 [87] also occurs in F_1F_0 [166], and that identical nucleotide-dependent conformational changes involving ϵ subunit occurred in F_1F_0 and isolated F_1 [46]. Nevertheless it is obvious that the catalytic mechanism is critically modified in the presence of a proton gradient, and a major goal for the future is to extend catalytic mechanism studies to intact F_1F_0-ATP synthase. For the present, however, we have to rely on evidence garnered mostly using isolated F_1.

There are six nucleotide-binding domains in F_1, three on the α and three on the β subunits, each of which has been defined in detail by X-ray crystallography as described in Section 2. The three nucleotide sites formed by the β subunits are the catalytic sites, and as the X-ray structure shows they lie at α/β subunit interfaces, with two residues from α subunit interacting with the nucleotide. Chemical inactivation with reagents such as DCCD and NBD-Cl, and (photo)affinity labeling experiments with nucleotide analogs, provided initial evidence that the catalytic sites were on the β subunits (reviewed in Refs. [1,115]). More definitive evidence has come from mutagenesis studies, in which specific mutations of residues in β subunit at conserved residues βK155 in the Homology A (P-loop) and βD242 in the Homology B sequence [167], were shown to drastically diminish catalytic activity, whereas the same mutations in α subunit did not [168–170].

Isolated β subunit does bind nucleotide, with a stoichiometry of 1 mol/mol [171–174]. However, when care was taken to ensure that there was no contamination of the isolated β subunit preparation by α subunit, it could be established that β alone does not hydrolyze MgATP at a significant rate [175], and thus it is not a useful experimental model for catalysis. Reconstitution experiments with isolated *E. coli* F_1 subunits showed that the minimal complex able to catalyse ATP hydrolysis at physiological rate is an $\alpha_3\beta_3\gamma$ complex [176]. This complex resembled F_1 in showing inhibition by azide [175] and the ability to bind and hydrolyse substoichiometric ATP by unisite catalysis [177]. It was shown that a complex of $\alpha\beta$ subunits from *E. coli* did have low but significant ATPase activity, in contrast to the negligible activity with either α or β subunit alone, but that the activity differed in characteristics from that of F_1 [175]. In CF_1 and TF_1 measurable hydrolytic activity has been reported for $\alpha_1\beta_1$ and/or $\alpha_3\beta_3$ assemblies

[178–182]; however, again these activities do not appear to be representative of the physiological mechanism, which is only seen in the $\alpha_3\beta_3\gamma$ complex. The high affinity catalytic site one was only seen in $\alpha_3\beta_3\gamma$ complex [178,183].

Thus, the portion of F_1 identified in the X-ray structure corresponds to the catalytic core of the enzyme and the huge amount of structural information resident in the X-ray structure analysis can now be applied to illuminate the catalytic mechanism. It is appropriate, however, to sound also a note of caution. In the X-ray structure, in one β subunit the nucleotide binding site contains MgAMPPNP (termed 'β_{TP}' in Ref. [13]), in the second β the site is filled with MgADP ('β_{DP}'), and the third catalytic site is empty ('β_E'). This pattern is presumably a consequence of the crystallization conditions (presence of Mg^{2+}, AMPPNP, ADP, azide; see Ref. [184]). There is now definitive evidence that all three catalytic sites are filled with nucleotide, MgATP and MgADP, during steady-state ATP hydrolysis (Section 4.4). The question arises therefore as to whether the enzyme form in the crystals is reflective of a physiologically-relevant state or whether it represents a non-physiological conformation. Consequently it seems premature to conclude whether the structure supports or does not support a given mechanism (see Ref. [185] for another opinion). We return to this point later.

4.2. The catalytic mechanism: an overview

At saturation with substrate MgATP, the steady-state hydrolysis rate of *E. coli* F_1 is 50–100 s^{-1} [99]; the mitochondrial enzyme can reach more than 500 s^{-1} [186]. When *E. coli* F_1 is assayed under appropriate conditions, a major fraction, if not all, of the MgATPase activity can be described by a single K_m value in the range of 100 μM [102]. Notwithstanding the fact that there is only a single apparent K_m(MgATP), steady-state catalysis involves all three catalytic sites, as will be documented below, and is therefore referred to as '*multisite*' catalysis. For ATP synthesis by *E. coli* F_1F_0 reconstituted into liposomes, a rate of about 30 s^{-1} was found; the substrate concentration dependence followed Michaelis-Menten kinetics with single K_m(ADP) of 27 μM, and $K_m(P_i)$ of 0.7 mM [164]. Chloroplast or mitochondrial F_1F_0 can reach substantially higher ATP synthesis rates [188,189].

At substoichiometric MgATP concentrations (i.e., non-steady-state conditions), the enzyme works in a quite different mode, referred to as '*unisite*' catalysis because it involves only a single catalytic site. Techniques for characterizing unisite catalysis were originally developed for the mitochondrial enzyme [190] and were modified for application to wild-type and mutant *E. coli* enzymes by Duncan and Senior [191]. Substoichiometric substrate MgATP is bound rapidly to catalytic site one with very high affinity ($K_d = 0.2$ nM for *E. coli* F_1, 1 pM for the mitochondrial enzyme) and is slowly hydrolysed to ADP plus P_i. The equilibrium constant for the chemical reaction is close to unity; thus this step is readily reversible even on the soluble enzyme. Release of products P_i and MgADP is very slow ($k_{off} \leq 10^{-3}$ s^{-1}). The four catalytic steps of unisite catalysis are ATP binding/release, ATP hydrolysis/resynthesis, P_i release/binding, and ADP release/binding. Rate constants for all steps except P_i binding may be directly measured, and have been reviewed [1,3,115,192]. The rate of P_i binding can be calculated from the product of the equilibrium constants at each catalytic step and the known overall $\Delta G^{\circ\prime}$ for ATP hydrolysis. Thus the unisite reaction can be completely described in kinetic and thermodynamic terms. It is because the P_i binding rate is negligibly slow (and consequently $K_d(P_i) > 1$ M) that synthesis of even enzyme-bound MgATP from medium P_i is impossible in soluble enzyme or non-energized membrane enzyme under ordinary conditions.

Given the ambient concentrations of MgATP in cells, unisite catalysis is obviously a non-physiological mode of operation of the enzyme. However, because it avoids complications introduced by the cooperative nature of the three catalytic sites, it has proven to be a valuable empirical tool. Unisite catalysis is insensitive to azide [193–195] consistent with its non-cooperative nature; the same unisite rate constants are seen in native or nucleotide-free enzymes, establishing lack of any effect of the noncatalytic sites in unisite catalysis [196]; and $\alpha_3\beta_3\gamma$ complex or ϵ-depleted F_1 show similar unisite behavior to intact F_1 [177,197]. There is excellent correlation between effects of catalytic site mutations on unisite catalysis and multisite ATP hydrolysis [163,169], and

conclusions regarding the location and possible function of various catalytic site residues derived from earlier studies of unisite catalysis were amply borne out by the X-ray structure when it appeared.

The highly-cooperative nature of the catalytic sites becomes obvious by comparing unisite parameters with those for multisite catalysis. For example if excess MgATP is added to *E. coli* F_1 performing unisite catalysis, occupation of additional catalytic sites leads to increase in net MgATP hydrolysis rate by five orders of magnitude, from $\leq 10^{-3}$ s^{-1} to 50–100 s^{-1} [191], and similar effects were seen in mitochondrial enzyme [3]. This positive catalytic cooperativity is accompanied by a similarly pronounced substrate binding cooperativity, for example K_d(MgATP) at catalytic site one differs from that at site three by at least five orders of magnitude. It is interesting to note that the strong catalytic cooperativity would have gone unnoticed if we had to rely solely on steady-state enzyme kinetic analyses. Such techniques have proved to be of limited value in studies of ATP synthase. They do not measure catalytic site occupancy directly, of course, and the results are often difficult to interpret in this highly-cooperative, three-site enzyme. In our experience, such kinetic measurements are prone to artifacts, including potent inhibition by free Mg^{2+} ions [187] or product (Mg)ADP [198,199], and 'lags' in initial rate when low concentrations of MgATP are used in conjunction with coupled enzyme optical assays. Boyer [200] has demonstrated how in a highly-cooperative enzyme, kinetic analyses are intrinsically subject to ambiguity of interpretation. Importantly, in a number of cases only a single apparent K_m value was observed [102,164], despite extensive evidence from other sources showing cooperativity between catalytic sites, demonstrating that K_m determination in isolation is no guide to the number of participating catalytic sites, nor their affinities.

The actual chemical reaction of MgATP hydrolysis is generally assumed to proceed by an in-line nucleophilic attack of a water molecule on the terminal phosphate, following an associative mechanism, and involving a pentacovalent phosphorus transition state [201]. Several pieces of evidence are consistent with such a mechanism. Two groups showed that the reaction proceeds with inversion of the configuration of the oxygen atoms about the terminal phosphorus, and that ADP-O is the acceptor for P_i in ATP synthesis, with no phosphoenzyme intermediate [202,203]. MgATP hydrolysis is strongly inhibited by fluoroaluminate [204], which mimics the pentacovalent phosphorus species occurring in the transition state [205,206].

4.3. Important advances from the study of unisite catalysis

Unisite catalytic parameters have been documented for bovine heart and yeast mitochondrial enzyme [3,207], and in *E. coli* enzyme by several laboratories [152,158,192,197,208] with good agreement. Soluble and membrane-bound forms of both mitochondrial and *E. coli* enzyme behave similarly [158,165]. The main differences between mitochondrial and *E. coli* F_1 are in K_d(MgATP) and K_d(MgADP), with the *E. coli* F_1 showing lower affinity by two orders of magnitude in both cases, and in the rate of MgATP hydrolysis and resynthesis ($k \sim 10$ s^{-1} in MF_1, 0.1 s^{-1} in *E. coli* F_1). The slower rate of hydrolysis in *E. coli* F_1 under unisite conditions allows manual methods to be used for measurements, with consequent ability to use small amounts of material, important for studies of mutants. Mutations usually reduce unisite rate constants, often very substantially. Increases are rarer, although one example was seen recently, in which a Cys residue was introduced in γ subunit in *E. coli* F_1, and then reacted with coumarin maleimide [152].

Several important advances have come out of studies of unisite catalysis. First, from a comparison of several enzyme species of widely-differing activity (mitochondrial, wild-type and mutant *E. coli*), it was apparent that F_1 utilizes binding energy derived from numerous side-chain to substrate interactions, which facilitate proximity, stereochemical orientation, immobilization and polarization of the substrate(s), as the major driving force for catalysis [163,169,192]. There may or may not be a specific catalytic base residue involved in catalysis, this point will be discussed below; but even if there is, it is certainly not the major driving force for catalysis. The binding energy utilized at each step of the unisite catalysis pathway has been quantitated, and a strong demonstrated correlation between unisite and multisite

catalysis shows that the same principles obtain also in the latter. Second, studies of unisite catalysis in the non-aqueous solvent dimethylsulfoxide or at pH varied from 5.5 to 9.5 confirmed that catalysis occurs in a hydrophobic environment which is sequestered from the medium. The chemical reaction steps are largely insensitive to ambient pH, although MgATP and P_i binding steps were both strongly pH-sensitive [99,209]. Third, construction of Gibbs free energy diagrams from the unisite reaction parameters allows the thermodynamic profile of the reaction to be visualized. From this emerges the conclusion that P_i binding and MgATP release are the major energy-requiring steps in ATP synthesis, which must be coupled to input of energy from the proton gradient, whereas MgADP binding occurs spontaneously. A model which describes how proton gradient energy is coupled to changes in the conformation of the catalytic sites was presented [163]. Fourth, Gibbs free energy diagrams provide a useful tool for comparison of enzymes from different species, and in particular for investigation of the effects of specific catalytic site mutations [163,169]. Several catalytic site functional residues have been characterized in this way, and will be discussed individually below.

The ^{18}O isotope exchange reactions reported previously in ATP synthases [210] are manifestations of reversible ATP hydrolysis and synthesis reactions occurring at catalytic site one. ^{18}O isotope exchange is apparent at low ATP concentrations, similar to unisite conditions [211,212]. The ^{18}O isotope exchange technique does not directly yield reaction rate constants. In earlier work [211] the assumption was made that the modulation of ^{18}O isotope exchange parameters which occurs on binding of excess MgATP is referable to binding of MgATP at a single additional catalytic site. With further assumptions, this allowed calculation of some catalytic rate parameters. However, it is now apparent that addition of excess MgATP leads rapidly to occupation of all three catalytic sites, not just two, and thus interpretation of the ^{18}O isotope exchange data is potentially very complex. Boyer [200] noted a discrepancy of two orders of magnitude between rates of ATP synthesis and hydrolysis as calculated from ^{18}O isotope exchange data and those determined directly in several laboratories from unisite experiments. Therefore the ^{18}O isotope exchange technique yields qualitative insights into catalysis, but is too ambiguous for determination of quantitative parameters. Similar reservations have been expressed in Ref. [213].

4.4. Nucleotide binding and hydrolysis in the catalytic sites: multisite catalysis

4.4.1. Multisite catalysis: two or three sites?

To describe multisite catalysis, numerous models have been proposed (e.g., Refs. [6,115,200,210,213–216]), most of which were adaptations or expansions of the 'binding change' or 'alternating site mechanism' proposed about 20 years ago [217–219]. Assumptions common to most of these models are: (1) The participating catalytic sites are in principle identical, but have, at any given time during catalysis, widely-different affinities for substrates and/or products. As a corollary, it was hypothesized that during catalysis the participating sites switch their properties in a synchronized manner. (2) One of these sites binds substrate and products tightly, and the chemical reaction is readily reversible in this site. Only this site is catalytically active at any one time. (3) Substrate binding at a second and/or third catalytic site is necessary for product release from site one. (4) In ATP synthesis, the energy from the proton gradient is used to decrease the affinity for ATP.

Supporting evidence for some of these assumptions has been presented [1,3,115,192,210,215]. In regard to points (2) and (4), the available evidence has been discussed above. As to points (1) and (3), until recently, there was no technique available to determine the occupancy or binding affinities of the individual catalytic sites under multisite catalysis conditions and on the time-scale of enzyme turnover. Conventionally-used methods to separate free from enzyme-bound ligand were either much too slow (equilibrium dialysis) or not true equilibrium methods (e.g., centrifuge columns). Not surprisingly, this was the place where the divergences between the models began. Pertinent experimental questions are therefore: How many of the catalytic sites, two or three, have to be occupied by substrate to achieve physiological catalysis rates? What is the actual affinity of each site for substrates and products? What is the distribution between bound MgATP and MgADP during catalysis?

There have been frequent attempts to determine

the number and affinities of catalytic sites on the basis of steady-state kinetic data. When the substrate concentration dependence of the catalytic activity could be better explained by two K_m values instead of one, the lower one was ascribed to 'bi-site' activity, the higher one to 'tri-site' catalysis. For reasons stated earlier, such conclusions are open to question.

4.4.2. Design and application of an optical probe to monitor occupancy of the catalytic binding sites

Recently, by inserting a tryptophan residue in position β331 of *E. coli* enzyme [102], we designed an optical probe which directly monitors occupancy of the catalytic sites by nucleotides. As can be seen in Fig. 4, this residue, which is tyrosine in mitochondrial and wild-type *E. coli* F_1, makes Van der Waals contact with the adenine ring of a catalytic-site-bound nucleotide molecule. βY331W mutant F_1 did not differ significantly in enzymatic characteristics from wild-type. The fluorescence signal of the three introduced βW331 residues was substantial, and readily visible over the background of the nine Trp residues present in wild-type. Its wavelength position indicated a very polar environment for βW331 when the catalytic site was empty. The X-ray structure shows the empty catalytic nucleotide binding site wide open; it is probably filled with water molecules. Upon binding of nucleotide, the fluorescence of residue βW331 is completely quenched. The fluorescence signal is the same for all three βW331 residues, and it is not affected by the status of occupancy of the noncatalytic sites [102,220]. Thus, βW331 fluorescence provides an ideal tool to measure thermodynamic and kinetic parameters for nucleotide binding to the catalytic sites. Table 2 summarizes data obtained using βW331 fluorescence, showing the

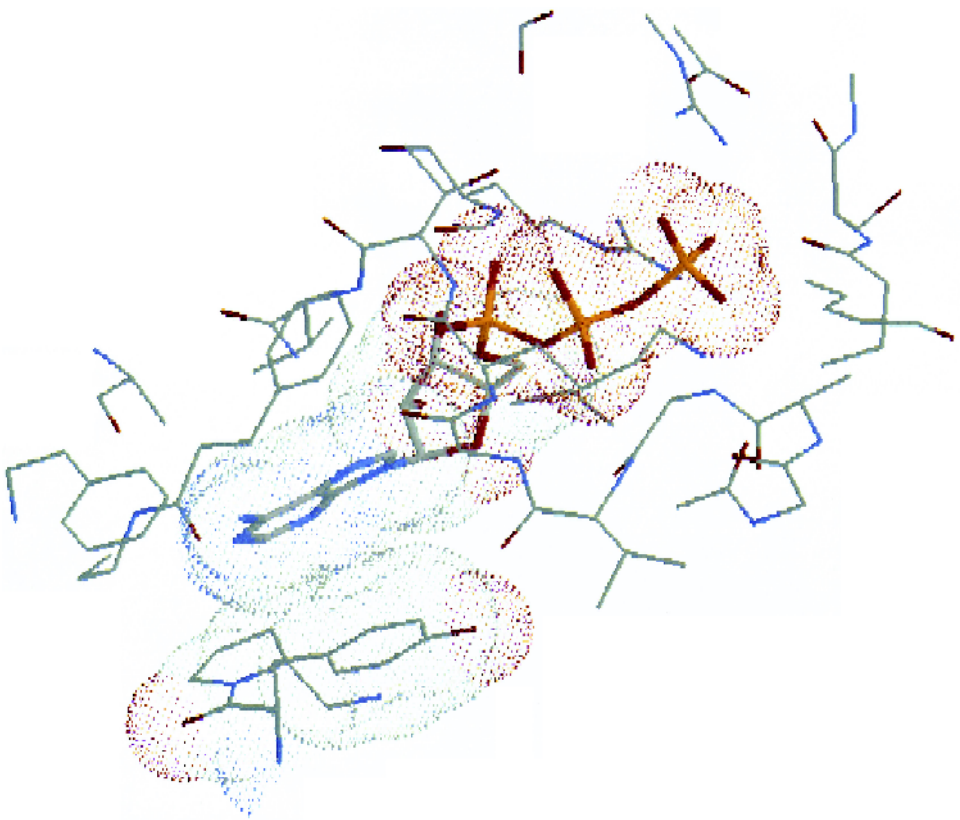

Fig. 4. Residue βY331 in the catalytic site makes Van der Waals contact with the adenine ring of bound nucleotide. The structure is that of the catalytic site which contains MgAMPPNP [13], displayed using RasMol. Van der Waals contact between residue βY331 and the adenine ring of the nucleotide is evident. The substitution βY331W yielded a probe in the catalytic site whose fluorescence is virtually completely quenched upon nucleotide binding, allowing monitoring of catalytic site occupancy during steady-state catalysis [102].

strong binding cooperativity of the catalytic sites for Mg-nucleotides, especially MgATP, and confirming that neither P_i (nor PP_i) shows significant binding to catalytic sites in the soluble enzyme.

Fig. 5A shows binding and hydrolysis of MgATP, measured under identical conditions over a wide range of MgATP concentration. A single K_m(MgATP) of about 40 μM is evident, and it is obvious that K_m(MgATP) is similar to K_{d3}(MgATP), the binding affinity of the third catalytic site. In Fig. 5C these data are replotted to show dependence of hydrolysis activity on fraction of catalytic sites filled, establishing that virtually all MgATPase activity was due to enzyme molecules having all three catalytic sites filled. The data show that, with MgATP, the activity of a molecule having just two sites filled is $\leq$ 2% of V_{max}, hence bi-site catalysis is without physiological relevance.

Fig. 5B shows binding and hydrolysis of MgTNPATP. Again it is seen clearly that all three catalytic sites have to be filled to reach V_{max}. When these data were replotted to demonstrate the dependence of hydrolysis activity on fraction of catalytic sites filled (Fig. 5D), it was apparent that, with MgTNPATP, substantial bi-site activity (38% of V_{max}) occurred. In absolute terms the rate of bi-site MgTNPATP hydrolysis was low, since even V_{max}(MgTNPATP) is less than 1.5% of V_{max}(MgATP) [103]. Nevertheless this experiment demonstrates that binding of nucleotide at catalytic site two can significantly accelerate catalytic rate, and opens the possibility that there may be a real albeit low level of bi-site MgATP hydrolysis also.

Comparison of the binding of MgATP and free ATP (Table 2) showed that Mg^{2+} is required for expression of catalytic site binding cooperativity and high affinity binding at catalytic site one. Fig. 6A,B shows binding curves for ATP and TNPATP obtained in the presence or absence of Mg^{2+}. In the absence of Mg^{2+}, all three catalytic sites bind ATP with the same affinity ($K_d = 71$ μM). It is interesting to note that this affinity is in the same range as that of the isolated β subunit for ATP or MgATP (25–100 μM [172,175,177,221]). There is no hydrolysis of free ATP by F_1 [220], nor is there hydrolysis of MgATP by isolated β subunit [175]. Thus, there is a correlation between formation of the high-affinity site one, catalytic site binding cooperativity, and catalytic activity. This correlation is also borne out by the data with MgTNPATP in Fig. 6B, which confirms that the presence of Mg^{2+} is mandatory for formation of the high affinity catalytic site one and the pronounced catalytic site binding cooperativity. It was also found that there is no hydrolysis of free TNPATP. This

Table 2
Nucleotide binding affinities and association rate constants at each of the three catalytic sites of *E. coli* F_1

Nucleotide	Binding affinity (K_d) (μM)			Association constant (k_{on}) ($M^{-1}\,s^{-1}$)		
	Site 1	Site 2	Site 3	Site 1	Site 2	Site 3
MgATP	0.0002 [a]	0.5	25	4×10^5 [a]	$\geq 2 \times 10^6$ [b]	2×10^6 [c]
MgTNPATP	$\ll$ 0.001	0.023	1.4	$> 5 \times 10^5$	2×10^7 [c]	8×10^5 [c]
MgADP	0.14	20	20	$\geq 5 \times 10^5$		
MgAMPPNP	0.11	36	36	6×10^3		
Mg*lb*ADP [d]	0.2	5.5	5.5			
free ATP	71	71	71			
free TNPATP	1.3	4.1	32			
AMP($\pm$Mg)	$>$ 1 000	$>$ 1 000	$>$ 1 000			
PP_i(+Mg)	$>$ 1 000	$>$ 5 000	$>$ 5 000			
P_i(+Mg)	$>$ 10 000	$>$ 10 000	$>$ 10 000			

All data were obtained using the fluorescence signal of residue βW331 except as indicated.
[a] Measured using radioactive MgATP and a hexokinase/glucose trap [196].
[b] See Ref. [220].
[c] k_{cat}/K_m for hydrolysis.
[d] Mg*lb*ADP, Mg-*lin*-benzo-ADP. The data were obtained from fluorescence of Mg*lb*ADP [232].

focusses attention on the critical importance of the catalytic site Mg^{2+} coordination ligands for both binding and catalysis.

Based on the results presented in Table 2, which show that $K_{d3}(MgATP) \approx K_d(free\ ATP) \approx K_m(MgATP)$, it cannot be excluded that during the catalytic cycle ATP is bound in the uncomplexed form at catalytic site three, and that only during the progress of catalysis, when site 3 becomes site 1 or 2, i.e., before the ATP is hydrolyzed, is Mg^{2+} bound into the ATP-filled site. For the time being, we see no convincing argument to prefer such a mechanism over the more reasonable one that catalysis involves MgATP exclusively.

Table 2 also documents that as far as thermodynamic and kinetic binding parameters are concerned, AMPPNP shows significant differences from ATP. It has been suggested that extreme stereochemical stringency, especially at the high-affinity catalytic site one, might be responsible for this behavior [222], and it is relevant to point out in this context that in the X-ray structure, catalytic sites were visualized with

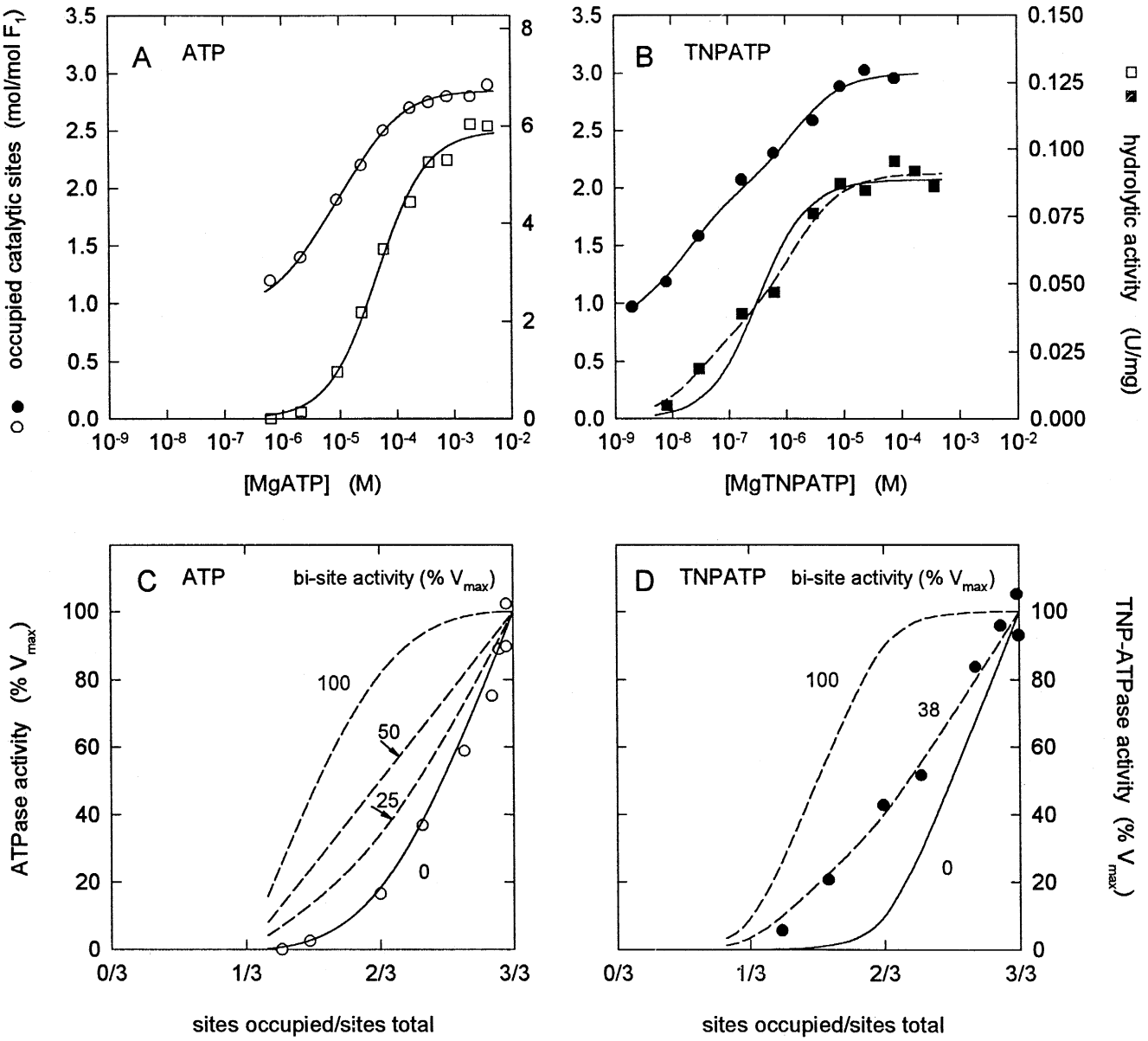

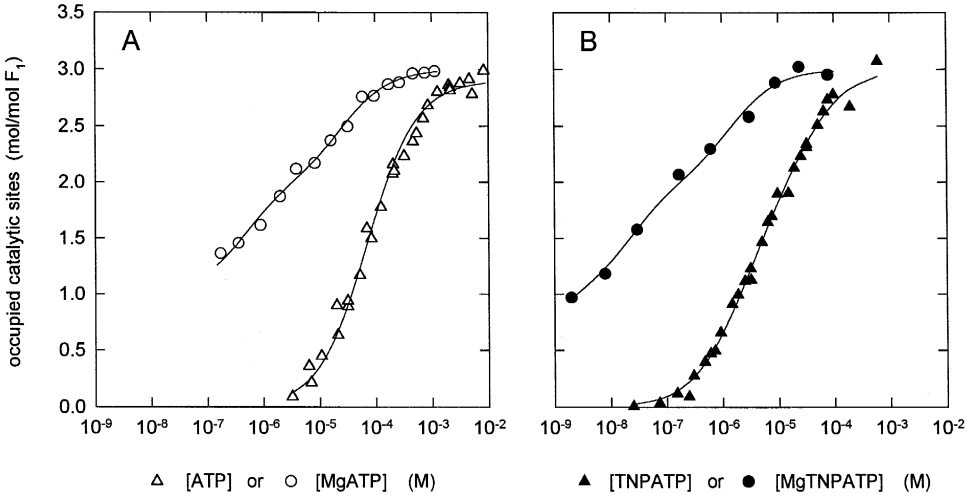

Fig. 6. Nucleotide binding cooperativity depends on Mg. Nucleotide binding to the three catalytic sites was determined using βW331 F_1 fluorescence. A: ATP in the presence (open circles) and absence (open triangles) of Mg. B: TNPATP in the presence (closed circles) or absence (closed triangles) of Mg. The binding affinities are shown in Table 2.

bound MgAMPPNP and MgADP, but not with bound MgATP.

4.4.3. Differentiation between catalytic site-bound MgATP and MgADP is made possible by the βW148 fluorescence probe and leads to a new model for multisite catalysis by F_1

Due to its location in the adenine-binding subdomain of the catalytic site, residue βW331 gives a nice response upon interaction with nucleotide but it is not able to differentiate between bound MgATP and bound MgADP. The ability to distinguish these two in real-time during catalysis is necessary for further dissection of the catalytic mechanism. We found that the introduction of a Trp into *E. coli* F_1 at residue β148, which immediately precedes the P-loop, yielded a fluorescent probe with the desired properties [223]. Upon binding of MgADP, the fluorescence of βF148W mutant F_1 was quenched, with maximum decrease at 350 nm. Upon binding of MgAMPPNP and MgADP · BeF_x (which is, like MgAMPPNP, isoelectronic and probably isosteric with MgATP; Ref. [205]) the fluorescence at 325 nm increased. With MgATP, both effects occurred simul-

Fig. 5. Catalytic site nucleotide binding and hydrolysis measured under identical conditions. A: MgATP binding (open circles) and hydrolysis (open squares) were measured under identical conditions using βW331 fluorescence assay and conventional P_i release assay, respectively, over the range of MgATP concentration shown. For hydrolysis a single K_m of 40 μM is apparent. From the binding curve it is seen that the first catalytic site is filled even at the lowest concentration of MgATP that can be used in the fluorescence assay, also that all three sites became filled, that there is strong binding cooperativity, and that the K_d at site 3 is similar to K_m. B: MgTNPATP binding (closed circles) and hydrolysis (closed squares) were measured as in panel A. MgTNPATP binds 20–30-fold more tightly than MgATP. Catalytic site one was already filled at the lowest MgTNPATP concentration used. There is strong binding cooperativity and all three sites had to be filled to reach V_{max}. The hydrolysis data could be fit using a single K_m (solid line) or two K_m values (dashed line); the latter gave significantly better fit. C: The data for MgATP binding and hydrolysis in panel A were replotted to show dependence of hydrolytic activity on catalytic sites occupancy. The open circles are the hydrolysis activity plotted against measured fraction of catalytic sites occupied (horizontal axis). The latter parameter is of course the average for all the enzyme molecules present. The solid line is the behavior expected if only molecules having all three catalytic sites filled show activity, i.e., bi-site activity equals zero. The dashed lines are the behavior expected if molecules with only two catalytic sites filled show 25, 50, or 100% of V_{max}. D: The data for MgTNPATP binding and hydrolysis from panel B were replotted to show dependence of hydrolytic activity on catalytic sites occupancy. The closed circles are the hydrolysis activity plotted against measured fraction of catalytic sites occupied (horizontal axis). The solid line is that expected if activity is seen only in molecules with all three catalytic sites occupied. The dashed lines are those expected if molecules with two catalytic sites occupied show an activity of 38% or 100% of V_{max}.

taneously, indicating that as added MgATP was hydrolyzed, both bound MgATP and MgADP were present on the enzyme [223]. The fluorescence responses were small (12–15%), and it was necessary to use tryptophan-free F_1 as background, so that βW148 was the sole tryptophan. Generation and properties of Trp-free F_1 retaining normal catalytic activity were described [224].

Using the βW148 fluorescence probe, we determined enzyme-bound MgATP and MgADP over a wide range of MgATP concentrations. At low MgATP (< 1 μM), when primarily the high affinity site one was occupied, the ratio of enzyme-bound MgADP to MgATP was about 0.5, which reflects the reaction equilibrium constant in unisite catalysis. Upon increasing MgATP (≥ 5 μM), catalytic site 2 became filled, nevertheless, the bound MgATP never exceeded 1 mol/mol F_1, indicating that MgATP in site 1 was rapidly hydrolyzed even though the overall turnover rate (i.e., product release) was still slow. At mM MgATP concentrations, i.e., V_{max} conditions ($K_m \approx 200$ μM for this mutant enzyme), all three catalytic sites were occupied as expected, and on average one of the three catalytic sites was filled with unhydrolyzed substrate MgATP and the two other catalytic sites were filled with product MgADP.

A new model for multisite MgATP hydrolysis encompassing these findings is shown in Fig. 7. The highest affinity catalytic site 1 is designated as 'H', the intermediate affinity site 2 as 'M', and the lowest affinity site 3 as 'L'. After release of MgADP from site L in the previous reaction cycle, site H is filled with MgATP and site M with MgADP (state D). Under V_{max} conditions, MgATP is rapidly bound to site L (state A). This promotes MgATP hydrolysis at site H, which in turn triggers a synchronized, concerted affinity change of the three catalytic sites (indicated by the arrows in state B). The subsequent release of P_i from the (now) site M is another fast reaction, resulting in state C. Release of MgADP from site L is the rate-limiting step of the multisite reaction cycle, hence state C is the most populous state of the enzyme molecules under V_{max} MgATP hydrolysis conditions. The essential advance contained in this new model is that it is based on actual measurements, on a real-time basis, of catalytic-site-bound MgATP and MgADP. The conclusion that MgADP release is the rate-determining step in multi-

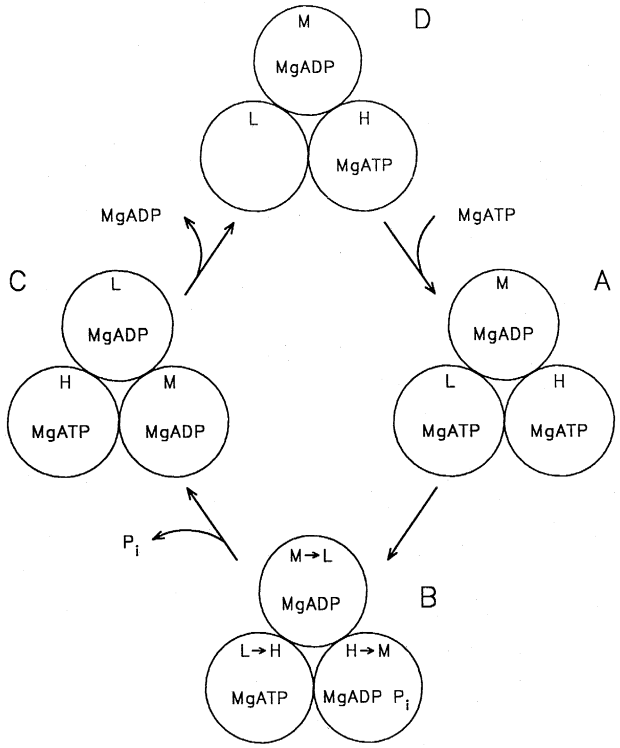

Fig. 7. Model for steady-state (multisite) hydrolysis of MgATP by F_1 deduced using the fluorescence of residue βW148. The three catalytic sites of the enzyme are depicted. H represents the site of highest affinity for MgATP (site one); M represents the site of intermediate affinity (site two); and L represents the site of lowest affinity (site three). During steady-state catalysis at V_{max}, the predominant form of the enzyme contains one bound ATP and two bound ADP, as in state C. The model is described in detail in the text.

site catalysis contradicts the postulate that substrate binding to one site and product release from another site occur *simultaneously* (see, e.g., Ref. [215]). If this were true, there would be no enzyme molecule with more than two sites filled at any given time during multisite catalysis. Obviously, data from both βW331 and βW148 enzymes show this is not the case. Substrate binding at one site is necessary for product release from a different site [218], and the two events are *synchronized* by the intervening affinity change; however, the binding step clearly precedes the release step.

Whether steady-state ATP synthesis can be described by simply reversing the reaction arrows in Fig. 7 remains to be determined. No direct measurements of catalytic site occupancy during ATP synthe-

sis, e.g., using optical probes, have been reported so far. Based on enzyme kinetic and radioactive nucleotide binding data, it has been proposed that in ATP or GTP synthesis all three catalytic sites have to be filled to obtain V_{max} rates [6].

In the X-ray structure of mitochondrial F_1 [13] one catalytic site is occupied with MgADP, a second with MgAMPPNP, and the third catalytic site is empty. This enzyme form could correspond to state D (Fig. 7), which in our model is a short-lived reaction intermediate during V_{max} hydrolysis. However, Grüber and Capaldi found in a recent study [156] that the lowest affinity catalytic site three resided on the β subunit which cross-linked preferentially to the γ subunit, whereas according to the X-ray structure, the β subunit whose residue βE380 is in contact with residue γC87 contains the catalytic site that is filled with MgAMPPNP, i.e., it is not the empty site [13]. These considerations reinforce our earlier point, that there are difficulties in relating the form of the enzyme seen in the X-ray structure to the active enzyme in solution.

4.5. Structure of the catalytic sites: the molecular basis for catalysis

4.5.1. X-ray structure and mutational analysis of the catalytic sites

The adenine-binding subdomain of the catalytic sites consists of side-chains of residues in and around helix 3 of the C-terminal domain of β subunit (βF404, βA407, βF410, βT411), and, to a large extent, of the aromatic ring of residue βY331 which is stacked with the adenine ring of the nucleotide (Fig. 4). βY331 had been identified earlier as part of the catalytic binding site by (photo)affinity labeling with a variety of nucleotide analogs. However, due to the different positions of the reactive group in these analogs [225–231], the precise spatial relationship of βY331 to bound nucleotide was unknown. Mutational analysis in combination with the use of a fluorescent nucleotide analog, *lin*-benzo-ADP, definitively located this residue as immediately adjacent to the adenine ring of the nucleotide [232]. The main function of βY331 is to provide an unpolar environment for the adenine ring; an aromatic residue is advantageous but not necessary for functional enzyme [232–234].

The ribose does not appear to make any specific interactions with the protein; the only residues that come relatively close are βF404 and βV157. The space around the ribose explains why even a large and rigid substitution at the ribose hydroxyls, as in TNPATP, is tolerated. In fact, TNPATP binds to *E. coli* F_1 20–30-fold more tightly than does ATP [103].

As in a variety of other nucleotide-binding proteins [205,235–239], the phosphates of catalytic-site bound nucleotide in F_1 are surrounded by residues of the P-loop [13], which in *E. coli* consists of residues βG149 to βT156 (GGAGVGKT). The most intimate contact is with the main chain atoms of βG152, βV153, and βG154, and with the side-chains of βK155 and βT156. The importance of the Gly residues in the P-loop is probably to accommodate to backbone conformational constraints, and some mutations of these residues fail to assemble an F_1-oligomer [169]. βG149 and βG152 can be replaced by small amino acids (βG149A, S; βG152A, C, S), but often with a significant loss in activity; the mitochondrial enzyme is less tolerant towards substitutions in position βG149 than the *E. coli* [240–242]. βG154 appears to be essential, but βG150 is tolerant of replacements [242].

Residues βK155 and βT156 have direct functions in nucleotide binding and catalysis. In position β155 not even arginine is tolerated and βT156 can only be replaced by Ser [169,207,222,242–245]. In unisite experiments with wild-type *E. coli* F_1, Al-Shawi and Senior [99] found that the affinity for both MgATP and P_i decreased markedly with increasing pH in the range 5.5 to 9.5; the pK_a for this effect was 8.0–8.4. In βK155Q and βK155E mutants the affinities for ATP and P_i were decreased by three orders of magnitude and were pH-insensitive. It was concluded that the side-chain of residue βK155 in wild-type lies very close to the γ-phosphate of ATP and to the position of P_i binding, and makes one or more specific hydrogen bonds with the γ-phosphate [222]. By providing significant binding energy, βK155 acts as a critical catalytic residue. The X-ray structure of the catalytic site (shown in Fig. 8) confirmed the predicted location of βK155, and demonstrated that the essential role of residue βT156 side-chain oxygen is to provide a coordination ligand to the Mg^{2+} of MgATP.

In addition to the P-loop, the immediate environ-

ment of the nucleotide phosphates consists of six charged residues, three acidic (βE181, βE185, and βD242) and three arginines (βR182, βR246, and αR376 from the adjacent α subunit) (Figs. 8 and 9). All of these residues appear to be important for function. The X-ray structure suggests that βE185 and βD242 (which is the last residue of the Homology B motif) are involved in binding the Mg^{2+} (Fig. 8), each probably via a water molecule. In both cases there is support for this proposal from mutational analysis [169,246]. Emphasizing the role of Mg^{2+} in catalysis, removal of either carboxyl group resulted in reduction of multisite hydrolysis rate by more than 3 orders of magnitude.

Abrahams et al. [13] found in the MgAMPPNP-containing catalytic site a density for a water molecule, hydrogen-bonded to the carboxyl group of βE181, 4.4 Å from the γ-phosphate. From spatial considerations, they proposed that βE181 might serve to activate the water molecule for an in-line nucleophilic attack on the γ-phosphate in ATP hydrolysis (see Fig. 8). Mutational analysis had already revealed the functional importance of βE181. Determination of unisite rate constants in βE181Q and βE181A mutant F_1 showed that the hydrolysis step on the enzyme was reduced by two orders of magnitude, that of the synthesis step by three [169,208,247]. Gibbs free energy diagrams of the unisite reaction pathway in βE181Q F_1 showed that the catalytic transition state was clearly the most affected species [169]. Further evidence for a special functional role for βE181 is provided by the fact that mutations of both βM209 [191,248,249] and βR246 [248,250] cause strong impairment of both multisite and unisite catalysis. It was concluded for both βM209I and βR246C mutants [163] that 'there is perturbation of the environment close to the site of catalysis'. From the X-ray structure the side-chains of both residues are seen to lie parallel to that of βE181, about 3 Å away from it, and pointing toward the γ-phosphate.

Residue αR376 approaches the nucleotide from the adjacent α subunit and comes close to the γ-phosphate (Fig. 9). It is interesting that this residue accounted for the most significant conformational difference between the MgAMPPNP-filled and the MgADP-filled site [13]. In the latter, it was shifted by 1.5 Å towards the β-phosphate. Abrahams et al. suggest this residue could serve to stabilize the penta-coordinate phosphorus catalytic transition state. In agreement with this, multisite ATPase activity was reduced by three orders of magnitude in the mutant αR376C [251,252]. In contrast, unisite catalysis appeared to be only slightly impaired; however, the rate constants that one would expect to decrease most upon loss of a side-chain stabilizing the catalytic transition state, namely those for the hydrolysis and synthesis steps, were not measured [251].

A number of residues located within a short stretch of α subunit have been identified as essential for multisite catalysis by random mutagenesis. The mutants obtained were αS347F, αG351D, αS373F, and αS375F [253,254]. Multisite hydrolysis in these mutants was strongly inhibited, but unisite catalysis was not greatly affected [193,255]. The mutations appeared to interfere with positive catalytic cooperativity between catalytic sites by interrupting a confor-

Fig. 8. X-ray structure of the catalytic site showing functional β subunit residues. The catalytic site with bound MgAMPPNP [13] (modelled in the coordinates as MgATP) is displayed using RasMol. The Mg atom is green. All the labelled residues in this figure are β subunit residues, that have been recognized as important for function by mutagenesis studies. βK155 and βT156 are the P-loop lysine and threonine, respectively. βD242 is the aspartate in the Homology B sequence, βE185 is a proposed Mg coordination ligand, and βE181 is the proposed catalytic base. See the text for further discussion.

Fig. 9. X-ray structure of the catalytic site showing the α/β interface and important α subunit residues. The catalytic site with bound MgAMPPNP [13] (modelled in the coordinates as MgATP) is displayed using RasMol. The Mg atom is green. α subunit residues are purple and are in the lower part of the figure. β residues (C atoms) are grey and are in the upper part of the figure. The α/β interface is obvious in this view. All the labelled residues in this figure are α subunit residues, that have been recognised as important for function by mutagenesis studies. Mutation of residues αG351, αS373 and αS375 blocks conformational signal transmission across the α/β interface which is critical for positive catalytic cooperativity and multisite catalysis. Residue αR376 is proposed to stabilize the transition state intermediate. See text for further discussion.

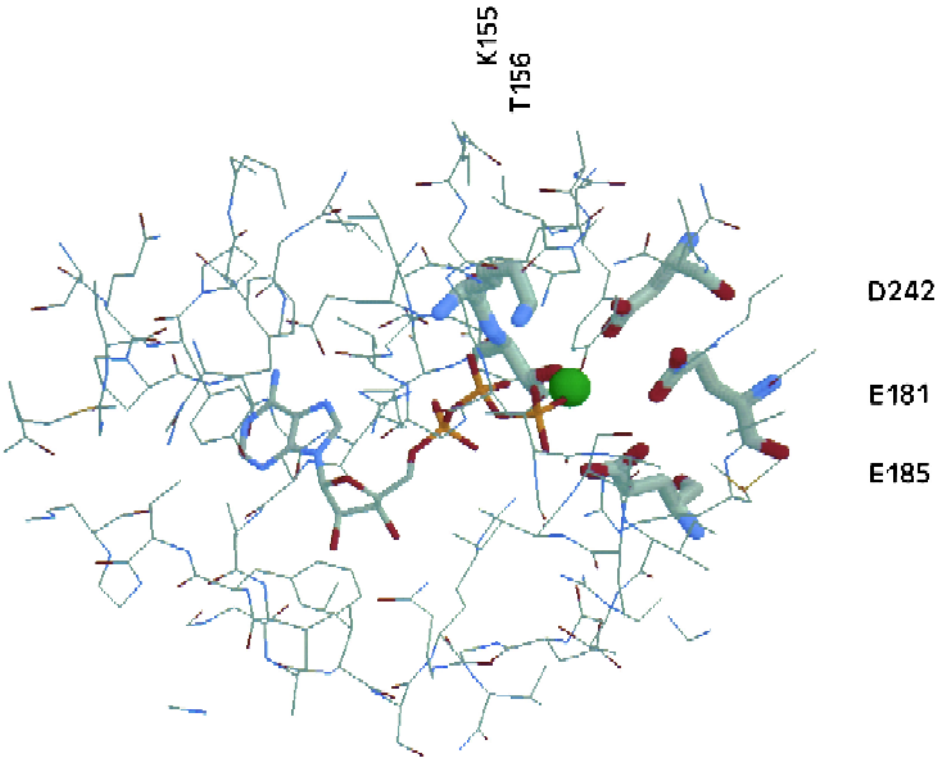

Fig. 8

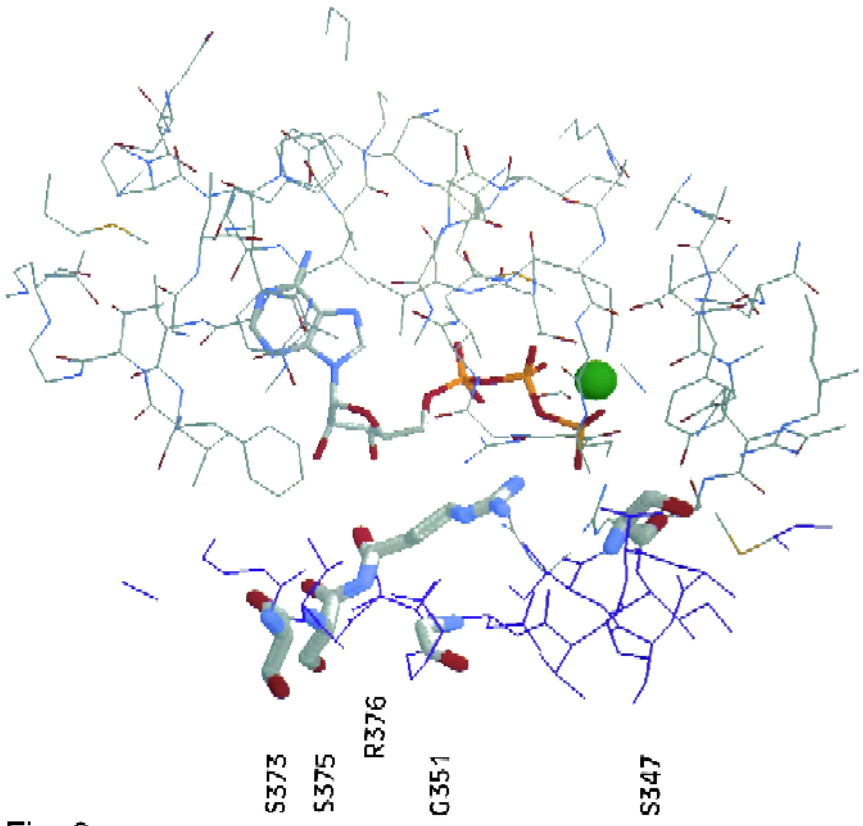

Fig. 9

mational interaction at an α/β interface, and this segment of α subunit was consequently termed 'α/β signal transmission region' [58]. Similar effects were seen in the αS373C mutant after reaction with NEM, and notably, reaction of only one NEM (mol/mol F_1) was sufficient to block multisite hydrolysis [256]. In a more recent study it was established that it is selectively the positive catalytic cooperativity that is blocked in these mutant enzymes; there is not a commensurate effect on nucleotide binding cooperativity [220]. Fig. 9 shows that all of these residues lie at the α/β interface in the catalytic site vicinity. In all cases, the substituted residue (or the NEM) is much bulkier than the original.

From the foregoing we propose the following mechanistic hypothesis. Residue αR376 makes contact with the pentacovalent transition state and is conformationally flexible. As the catalytic hydrolysis event proceeds, αR376 is impelled to move, this movement is amplified by the α/β interface and transmitted to the proximate α subunit. The conformational movement is then propagated to the other catalytic sites and it triggers the switching of their affinities as shown in step B of Fig. 7. From previous discussion it is evident that α, γ, and ϵ subunits are all involved in propagation of this conformational signal. The substitution of bulky residues at the α/β interface close to the catalytic site freezes the molecule, such that nucleotide binding cooperativity is still seen, but the switching of catalytic site binding affinities that leads to release of product cannot occur (see Fig. 7). The finding that reaction of NEM at only one of the α/β interfaces still blocks multisite catalysis [256] strongly supports a cyclical mechanism as in Fig. 7. Presumably in coupled ATP-driven proton transport, the conformation change induced by the hydrolysis event is transmitted through the γ and the ϵ subunit to the *c* subunit (Section 3).

4.5.2. Binding energies and catalytic site binding affinity changes

A dissociation constant (K_d) of 0.2 nM, as found for MgATP binding at catalytic site one in *E. coli* F_1, corresponds to a $\Delta G^{o\prime}$ of $\sim$13 kcal/mol; a K_d of 100 μM (the approximate K_d for MgATP at catalytic site three) to a value of $\sim$5.5 kcal/mol. This energy must be generated by multiple interactions between the protein surface and the nucleotide. The difference of $\sim$7.5 kcal/mol has to come from those parts of the binding site that are responsible for the differences in binding affinity between the catalytic sites. These are the specific interactions that engage and disengage as the sites switch affinity during the catalytic cycle. Regarding ATP synthesis, it was found that the presence of a proton gradient alone facilitated ATP dissociation from the high-affinity site one of MF_1F_0, equivalent to a standard free energy change of 8 kcal/mol; in the presence of ADP and P_i, the respective value was closer to 10 kcal/mol [159,160]. About 10 kcal/mol will also be necessary to reduce the binding affinity of the high-affinity site in the *E. coli* enzyme to a level corresponding to the intracellular ATP concentration, as discussed in Section 3. In the following, we will try to identify some of the residues which contribute binding energy to the interaction between enzyme and nucleotide, and discuss how changes in affinity of a catalytic site during ATP hydrolysis or synthesis can be brought about.

The adenine binding subdomain provides a hydrophobic environment for the adenine ring. The contribution of the side-chain of βY331 can be estimated from *lin*-benzo-ADP binding data [232]. If we take the βY331A mutant as standard (i.e., assuming no interaction between alanine and the adenine ring), the contribution of the tyrosine to the binding affinity at catalytic site 1 is equivalent to 1.5 kcal/mol. From data obtained with other β331 mutants (F, L, W), it can be calculated that the contribution of this residue is the same in all three catalytic sites. Information about other adenine ring binding side-chains is unavailable as yet. As noted above, no specific interactions between the protein and the ribose moiety are evident. The only information we have in this regard comes from TNPATP binding experiments [103]. Addition of the trinitrophenyl moiety to ATP increases the binding affinity at all three sites by the same factor. Therefore, from the available and admittedly incomplete data, the parts of the catalytic site which bind the adenine ring and the ribose do not appear to be involved in changes in binding affinity and contribute little to the overall binding energy. Consistent with this, binding of AMP is negligible [220].

This leaves the phosphate binding pocket as the major source of binding energy. From the dissocia-

tion constants obtained in unisite experiments with wild-type and mutant enzymes [169], it can be calculated that residue βK155 contributes 3.9 kcal/mol to MgATP binding at the high affinity catalytic site 1, but only 0.6 kcal/mol to MgADP binding. Using a βK155Q/βY331W double mutant, we were recently able to estimate the respective values for catalytic sites 2 and 3 from fluorescence titration data (S. Löbau, J.W. and A.E.S., unpublished results). These are 3.4 and 1.1 kcal/mol for MgATP binding to sites 2 and 3, respectively, and ~0 kcal/mol for MgADP at both sites. The results are those expected if residue βK155 is in direct contact with the γ-phosphate of bound MgATP, at least at sites 1 and 2. The reduced interaction between this residue and the γ-phosphate at site 3 seems largely responsible for the differences in affinity for MgATP between sites 2 and 3. We envisage that movement of this residue away from the γ-phosphate ('disengagement'), is one contributor to proton gradient-induced, energized release of MgATP in oxidative phosphorylation.

It is obvious from Fig. 6 and Table 2 that in intact F_1 a critical determinant of catalytic site binding affinity and cooperativity is Mg^{2+}. In the absence of Mg^{2+} all three sites bind ATP with K_d of around 70 μM; in its presence catalytic site three remains of a similar affinity, but catalytic sites one and two both become tighter, indeed site one achieves a K_d of 0.2 nM. Thus Mg^{2+} coordination is a major component of binding energy and of affinity changes. The Mg^{2+} of MgATP is expected to have six coordinating ligands. Abrahams et al. [13] suggest that one is the βT156 hydroxyl oxygen and two are oxygens of the β- and γ-phosphates. One other is a water molecule which is hydrogen-bonded to residue βD242 (Fig. 8; Ref. [169]; and Leslie, A.G.W. and Walker, J.E., personal communication), and a fifth is probably a water molecule hydrogen-bonded to residue βE185 (Fig. 8 and Ref. [246]). The sixth might be the hydroxyl of residue αS347 [257] which approaches the Mg^{2+} in the catalytic site. Given the data of Fig. 6, it follows that a major difference between catalytic sites one and three resides in the degree of engagement of Mg^{2+} ligands, and that proton gradient-induced release of MgATP into the surrounding milieu requires disengaging them.

Unfortunately, for the calculation of binding energy contributed by the proposed Mg^{2+}-coordinating residues, only data for the carboxyl group of βD242 at catalytic site 1 exist [169]. For MgATP the value is 3.0 kcal/mol. A clear goal of future research is to establish the identity of all the Mg^{2+} ligands, calculate their contribution to overall binding energy, and define their role in binding affinity changes.

In conclusion, from presently available mutational data, the phosphate binding pocket is not only responsible for the reaction chemistry, but also for the bulk of the binding energy with MgATP, and for the affinity changes during multisite catalysis. This is strongly supported by the observation that presence of the proton gradient increases the affinity for substrate P_i by several orders of magnitude, without significantly affecting that for MgADP (above), indicating that energization results in localized structural changes in the environment of the P_i. For further understanding it seems imperative to obtain a high-resolution structure of the high-affinity catalytic site filled with MgATP. MgAMPPNP appears to be no good substitute for this purpose, as the affinity of catalytic site 1 for MgAMPPNP is about 3 orders of magnitude lower than that for MgATP (Table 2).

4.5.3. Is there a catalytic base and if so is it residue βE181?

From the position of residue βE181 in the catalytic site (Fig. 8), Abrahams et al. [13] suggested that it may function as a general base to activate the neighboring bound water by abstracting a proton. One lesson we can learn from the experiences with a variety of other nucleoside triphosphate-hydrolyzing proteins is that a general base residue is not necessary. Perhaps the best-investigated example is p21*ras*. Originally, it was proposed that residue Q61 is the catalytic base in this protein, and that it was assisted in this role by E63 [258,259]. Later experimental results [260] as well as theoretical considerations [261] made this concept untenable. Instead, a mechanism was suggested recently where the γ-phosphate of bound GTP itself is the catalytic base [262], and possible functions of Q61 include stabilizing the transition state by making hydrogen bonds to the nucleophile OH^-, and/or to one of the phosphate oxygens [263]. A similar mechanism where, however, the proton is not transferred directly to the γ-phosphate but via Q200 (equivalent to Q61 in p21*ras*) has been suggested for transducin α [206].

It has been argued that the absence of a general base residue might be characteristic of hydrolytic sites with a slow turnover rate [264]. However, in the presence of GTPase activating proteins, the hydrolytic activity of p21*ras* reaches 20 s^{-1}. In myosin, the rate constant for the hydrolytic step is even higher [265], yet the X-ray structure of *Dictyostelium discoideum* myosin subfragment 1 complexed with $MgADP \cdot BeF_x$ did not reveal any amino acid side-chain within 5 Å of the beryllium (which is in the position of the γ-phosphorus of ATP) that could act as catalytic base [205]. These authors suggested two possible mechanisms for myosin ATPase, one with direct proton transfer from the water molecule to the γ-phosphate (analogous to Ref. [263]), and an alternative one where such a transfer occurs via a serine (analogous to Ref. [206]).

So far, the experimental evidence regarding the function of residue βE181 in the catalytic site of F_1 is consistent with a role of this residue as general base, but in reality the same evidence supports any model which attributes to βE181 an important function in the catalytic reaction step. It may be noted that studies of the pH-dependence of unisite catalysis showed that the MgATP hydrolysis and resynthesis rates were unaffected over the pH range 5.5 to 9.5, i.e., no functional side-chain with $pK_a \geq 5.5$ was evident. One possibility, which we favor, is that βE181 serves to stereochemically align and to polarize the water molecule for the nucleophilic attack, via hydrogen bonding to the (charged) carboxyl, without actual proton abstraction. Even if βE181 is acting as general base, it should be noted that removal of the carboxyl group in βE181Q mutant F_1 reduced V_{max} for multisite hydrolysis by three to four orders of magnitude [169,208]. This means that the mutant enzyme still accelerates ATP hydrolysis by a factor of more than 10^6. Thus, the major part of the acceleration of catalysis has to come from the binding energy from multiple protein-to-nucleotide interactions. One observation of note is that the carboxyl of βE181 is differently-positioned in each of the three catalytic sites in the X-ray structure. Only in one site is it directly in-line with the (presumed) attacking water and the γ-phosphate. This, together with different binding affinity of the three sites, could explain why only one of the three catalytic sites would be catalytically-competent at any given time. As noted earlier, this point, although not experimentally proven, is implied in all current models.

4.6. Summary

Specific placement of tryptophan residues into the catalytic nucleotide binding sites as optical probes to monitor occupancy of the sites has greatly improved functional characterization. The pronounced binding cooperativity between catalytic sites is Mg^{2+}-dependent, as is catalytic turnover. For MgATP hydrolysis at V_{max} rates, all three catalytic sites have to be filled. Under these conditions, in average over all enzyme molecules, one of the three catalytic sites is filled with unhydrolyzed substrate MgATP, the other two with product MgADP. A new model for MgATP hydrolysis is presented, based on important features of earlier models and encompassing the new measurements.

A major recent development in the investigation of the catalytic mechanism was the arrival of a structural model of F_1 based on X-ray crystallography. The X-ray structure was able to explain and clarify many earlier findings, and will undoubtedly inspire the design of new experiments. As one result, and in combination with the results of earlier mutational analysis, the function of specific amino acid residues in the catalytic binding domain is now emerging. Binding energy from these residues is the major driving force for catalysis; calculation of the binding energy contributed by individual side-chains is now feasible and ongoing.

Among the important questions: (1) What is the molecular basis for the widely-differing affinities of the three catalytic sites, which is manifested as binding cooperativity? (2) What is the molecular basis for the binding affinity changes which occur during hydrolysis and which generate the phenomenon of positive catalytic cooperativity? (3) What is the molecular basis for the affinity changes necessary to decrease MgATP affinity and increase P_i affinity upon generation of a proton gradient, and how is MgATP re-binding prevented? (4) Does a general catalytic base exist and what, if any, is its quantitative contribution to catalysis? Each question represents one facet of the complex, delightfully intriguing, catalytic mechanism of F_1.

5. The three noncatalytic nucleotide-binding sites

5.1. Structure and general properties

Isolated α subunit binds both ATP and ADP tightly with 1/1 stoichiometry [171,173,176,266,267], thus it was no surprise that in the X-ray structure of F_1 the three α subunits were seen to be each binding one molecule of nucleotide MgAMPPNP [13]. When nucleotide-free F_1 is loaded with radioactive MgAMPPNP, initially all six nucleotide sites bind the ligand, but after removal of medium MgAMPPNP and further incubation with 1 mM MgATP or 10 mM MgADP, three nucleotide sites retain MgAMPPNP for hours [268]; these three sites, which are clearly quite nonexchangeable, were dubbed 'noncatalytic sites' [269]. They correspond to the sites which, in membrane F_1F_0 preparations or purified F_1, are filled with endogenous ATP and ADP [270]. Confirmation that these sites are truly not catalytic came from the demonstration that bound [γ-^{32}P]ATP remains unhydrolysed for long periods [271] (see also Ref. [272]). The evidence that it is the three α subunit nucleotide sites which correspond to the noncatalytic sites (as opposed to the three nucleotide sites on the β subunits) comes from mutagenesis studies, in which mutations were introduced in both α and β subunits at the highly-conserved P-loop Lys residues and Homology B Asp residues. Whereas these mutations drastically impaired catalytic activity

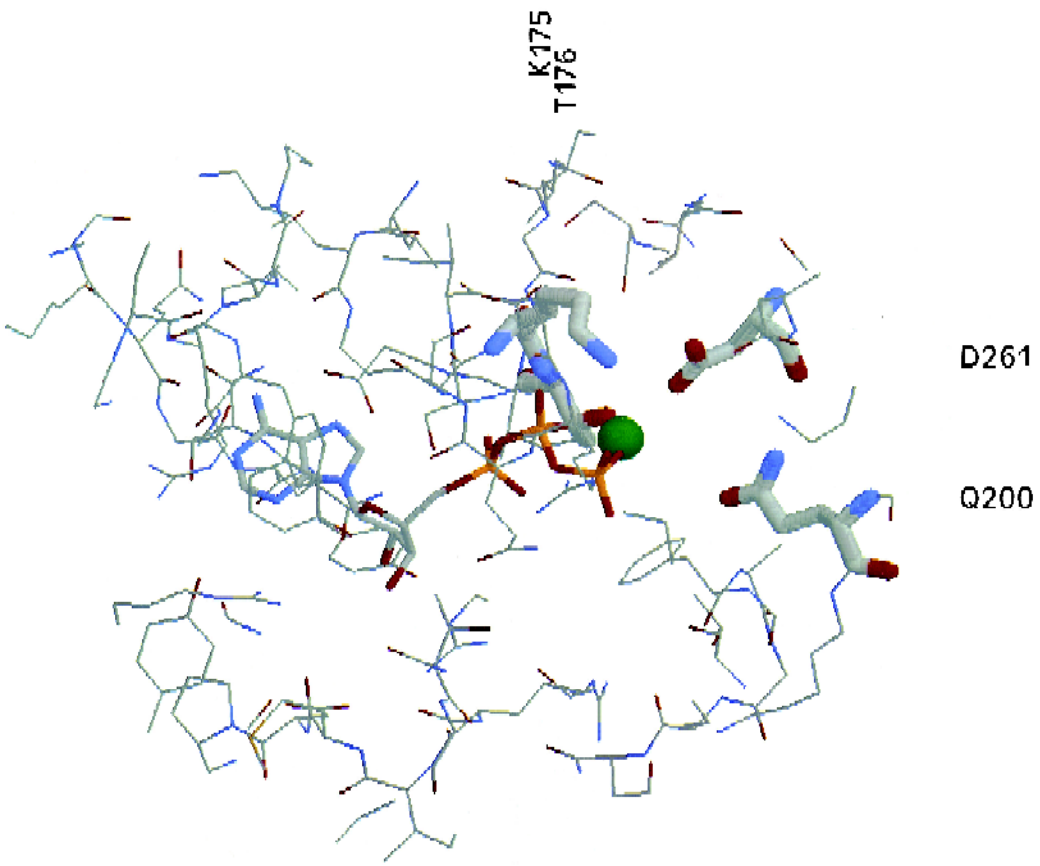

Fig. 10. X-ray structure of the noncatalytic site. The structure is that determined for bovine heart mitochondrial F_1 subunit α_{DP} [13], displayed using RasMol, with MgATP modelled as the bound nucleotide instead of MgAMPPNP actally present in the crystals. The Mg atom is green. All the labelled residues in this figure are α subunit residues. αK175 and αT176 are the P-loop lysine and threonine, respectively; αD261 is the Homology B aspartate; and αQ200 is equivalent to the proposed catalytic base residue βE181 of the catalytic sites.

when placed in the β subunits, the same mutations in the α subunits had small effects [168–170]. Further evidence on this point is reviewed in Ref. [273].

In general the catalytic and noncatalytic nucleotide sites are similar in architecture [13], consistent with the fact that α and β subunits are homologous throughout their sequences. Fig. 10 shows the structure of the noncatalytic site as derived by X-ray crystallography. In this figure the nucleotide was modelled as MgATP, although in the crystals MgAMPPNP was the actual ligand. Around the nucleotide we have highlighted several α subunit residues of interest. αK175 is close to the γ-phosphate, and previous mutagenesis work had shown that nucleotide binding was an important role of this residue [168]. The oxygen of the αT176 hydroxyl ligates to the Mg atom. αD261 appears to ligate indirectly to the Mg atom through a water molecule, and mutagenesis of this residue has confirmed its role in conferring Mg-dependence of nucleotide-binding (see below). Residue αQ200 is in the position equivalent to the putative catalytic residue βE181 of the catalytic sites, discussed in Section 4. In two noncatalytic sites the side-chain of αQ200 points towards the γ-phosphate, in the third (α_{TP}, using the terminology of Ref. [13]) the side-chain of αQ200 points obliquely away from it.

The noncatalytic sites, although obtaining the majority of their nucleotide-protein interactions from α subunit side-chains, also lie at α/β interfaces. In subunit α_E [13] two residues from subunit β_{DP} protrude into the nucleotide site (βR358 and βY354); in subunit α_{DP} only βY354 interacts with nucleotide; and in subunit α_{TP} no residues from β are part of the noncatalytic site. Residue βY354 is the residue labeled by the nucleotide analogs FSBA and 2-azido-ATP when bound in noncatalytic sites [226,227,274], reflecting the selectivity of these reagents for tyrosyl side-chains [273]. Inhibition of ATP hydrolysis by these labels [226,273,274] reflects freezing of α/β conformational interactions by 'cross-linking' across the α/β interface, as was predicted [173].

It is interesting to ask why these sites do not hydrolyze MgATP. Abrahams et al. [13] suggest one reason, namely that in α subunits, residue αQ200 is equivalent to the putative 'catalytic base' residue (βE181) of the catalytic sites and lacks the essential

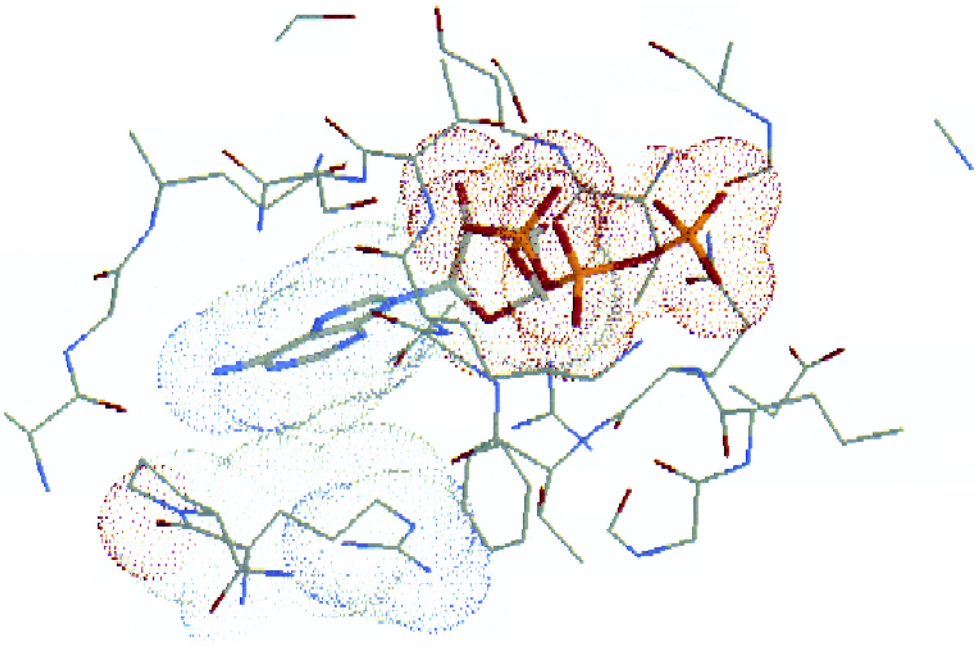

Fig. 11. Proximity of residue αR365 to the adenine ring of bound nucleotide in the noncatalytic site. Van der Waals radii are drawn around the adenine ring of bound nucleotide and the side-chain of the wild-type residue αR365 in the noncatalytic site. As discussed in the text, the substitution αW365 yields a direct fluorescence probe of nucleotide binding to noncatalytic sites.

carboxyl. However, as we note above, the mutation βE181Q decelerates ATP hydrolysis by about 1000-fold, but does not abolish it. Matsui and colleagues found that the mutation αQ200E allowed some hydrolysis of 'tethered' 2-azido-ATP, but there was no significant hydrolysis of MgATP [272]. Therefore, there must be additional reasons for the lack of catalysis in noncatalytic sites.

5.2. Recent work on characterization and function of noncatalytic sites

Older studies aimed at characterization of noncatalytic sites utilized mainly a technique consisting of preincubation of the enzyme with radioactive nucleotide, followed by 'chase' with a ligand designed to displace nucleotide from catalytic but not from noncatalytic sites, then passage through a centrifuge column to separate bound from unbound radioactive nucleotide. Remaining bound ligand was assumed to reside in noncatalytic sites. The technique has the limitations that it is not a true equilibrium binding method, and is subject to artifacts, namely (1) the ligands GTP and PPi, previously used to displace catalytic site bound-nucleotide, turn out to lack specificity for binding to the catalytic sites, and (2) with MF_1 and CF_1, MgADP bound to catalytic sites may be mistaken for noncatalytic site-bound ligand, particularly where short 'chase' times are used to displace catalytic site nucleotide.

A recently introduced technique utilizes the fluorescence of an inserted tryptophan residue, αW365, to monitor occupancy of noncatalytic sites [34]. This is a true equilibrium method and measures noncatalytic site nucleotide-binding specifically. The αR365W mutant enzyme shows normal catalytic properties. In the X-ray structure of the noncatalytic sites the aliphatic side-chain of wild-type residue αR365 approaches the adenine ring of bound nucleotide, with the guanidinium group pointing away from the adenine. As Fig. 11 shows, the Van der Waals radius of the adenine ring of bound nucleotide overlaps with that of the side-chain of residue αR365, explaining why the fluorescence of the introduced αW365 provides a sensitive and unambiguous probe.

The three noncatalytic sites are of essentially equal affinity for MgATP, MgADP and MgAMPPNP, and there is no cooperativity of binding (Table 3)

Table 3
Nucleotide binding affinity at the noncatalytic sites in *E. coli* F_1

Nucleotide	Binding affinity (K_d) (μM)
MgATP	25
MgADP	24
MgAMPPNP	16
MgAMP	>2000
free ATP	3500
free ADP	1300
PPi (+Mg)	20
Pi (+Mg)	>10000
MgGTP,MgITP	≈ 1000
MgGDP,MgIDP	>5000

The binding affinity was the same at all three noncatalytic sites. For MgATP the association constant (k_{on}) was measured and was 270 M^{-1} s^{-1} at all three sites.

[34,162,170]. The association rate constants of these nucleotides are quite slow, for example, 270 M^{-1} s^{-1} for MgATP, which is ≥ 3 orders of magnitude slower than binding to the catalytic sites. Binding of all three nucleotides was Mg-dependent, the K_d for free ATP was >1 mM [34,162]. Mg^{2+} confers greatly increased binding affinity on ATP and ADP primarily due to interaction with residue αD261 of the Homology B sequence, which contributes ~ 3 kcal/mol of binding energy [170]. Fig. 10 shows the close proximity of the Mg atom to the residue αD261 carboxyl group. AMP, GDP and IDP do not bind to noncatalytic sites, but (contrary to what was concluded from previous work [275]) GTP and ITP are bound to some extent [34]. PP_i is remarkable in that it binds relatively tightly ($K_d = 20$ μM) to noncatalytic sites, but not significantly to catalytic sites [162,276–279]. P_i does not bind to noncatalytic sites [162].

Using PP_i as a 'trap' to prevent nucleotide from re-binding, it was possible to study the rate of dissociation of nucleotide from noncatalytic sites [162]. Mutant F_1 containing residue αW365 was first rendered nucleotide-free, then incubated with MgATP. The tryptophan fluorescence signal recorded the initial binding of nucleotide, which yields State I of Fig. 12, in which nucleotide is bound with the same affinity as PP_i, indicating it is the 'pyrophosphate' end of the nucleotide that is first recognized. Then the enzyme was diluted into PP_i-containing buffer. Since PP_i binds to noncatalytic sites but does not

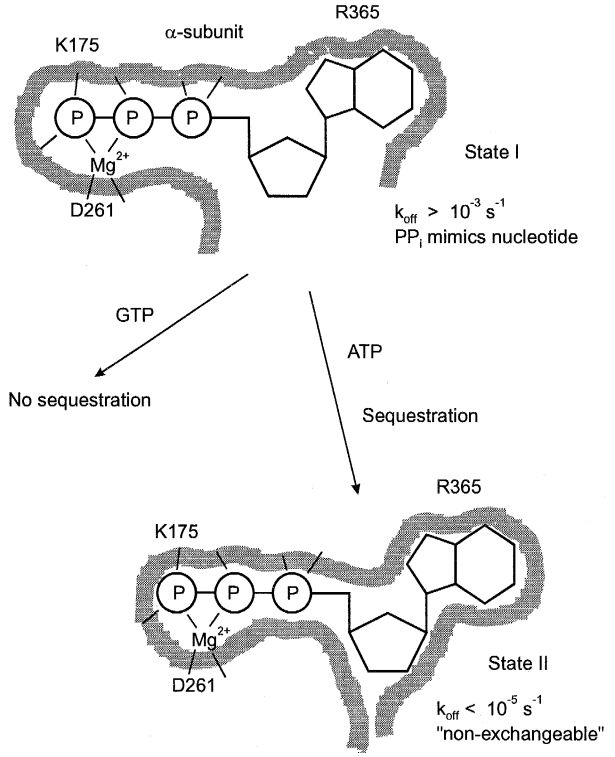

Fig. 12. Scheme for sequestration of adenine nucleotide in the noncatalytic sites. Initial binding of nucleotide in the noncatalytic sites appears to involve the 'pyrophosphate' end of the molecule, and leads to State I, which has relatively fast k_{off}. If the nucleotide is MgATP, there is then a slow conformation change to State II. In State II adenine nucleotide is sequestered, k_{off} is very slow. This is the physiological state of the enzyme, hence the tenacious binding of the endogenous adenine nucleotide in the native enzyme. Sequestration does not occur with GTP (or ITP), explaining the apparent preference of the sites for adenine nucleotide.

quench the fluorescence of residue αW365, an increase in fluorescence monitors dissociation of nucleotide. The apparent dissociation rate constant (k_{off}) for MgATP measured immediately after dilution was $> 10^{-3}$ s^{-1}. Over a period of hours the apparent MgATP dissociation rate constant decreased significantly, indicating that a slow conformational change occurred which led to State II of Fig. 12, in which MgATP is sequestered and rendered non-exchangeable. Indeed, with 'native' enzyme (i.e., enzyme never subjected to the nucleotide-depletion procedure) the release rate of endogenous adenine nucleotide from the noncatalytic sites was $< 10^{-5}$ s^{-1}.

In contrast, on addition of MgGTP, initially occupancy of noncatalytic sites was seen, but the dissociation rate was fast (> 0.1 s^{-1}), and it did not change with time. Hence, there was no sequestration of MgGTP (Fig. 12). Therefore there is an apparent preference of the noncatalytic sites for adenine vs. guanine (and inosine) nucleotide, as was seen in earlier work [275], which is reflected in the different dissociation rates. Abrahams et al. [13] concluded from the X-ray structure that sequestration of adenine nucleotide in noncatalytic sites results from formation of several H-bonds between α subunit side-chains and the adenine ring.

What is the function of the noncatalytic sites? Is there indeed any function? None has yet been demonstrated. In regard to the ATP synthesis reaction, earlier work [280] using *E. coli* F_1F_0 in membranes showed that GTP synthesis from GDP by oxidative phosphorylation occurred at similar rates whether the noncatalytic sites were empty, or filled with ATP, ADP or AMPPNP. These conclusions remain valid. More recently [281], it was shown that ATP synthesis by TF_1F_0 reconstituted in proteoliposomes occurred at a significant rate when the noncatalytic sites were empty, but that the rate increased by 2–3-fold when the sites were occupied by adenine nucleotide. Thus, occupancy of the sites improved enzyme efficacy in the in vitro system. The effect was maximal at 10 μM added ATP, however, which is far below cellular ATP concentration. In αD261N mutant *E. coli* enzyme, MgATP and MgADP binding to noncatalytic sites was drastically weakened, such that purified F_1 contains empty noncatalytic sites [170]. Nevertheless, oxidative phosphorylation was normal in this mutant in vivo.

Similar considerations apply to the ATP hydrolysis reaction. Occupancy of the noncatalytic sites had no effect on unisite catalysis [196]. *E. coli* F_1 containing MgATP, MgADP, MgAMPPNP or PP_i bound at noncatalytic sites showed similar multisite V_{max} activity [162,280]. Experiments which exploited the fast rate of MgATP binding to catalytic sites as opposed to the slow rate of binding to noncatalytic sites, showed that the enzyme hydrolyzed MgATP at similar rates whether the noncatalytic sites were occupied or not [34]. Furthermore, αD261N mutant enzyme showed no diminution of ATPase activity at nucleotide concentrations insufficient to give significant occupation of noncatalytic sites [170].

5.3. Summary

The technique of specific insertion of tryptophan to provide a direct fluorescence probe has allowed extensive characterization of the noncatalytic sites. However, no essential functional role for the noncatalytic sites is evident, and a physiologically-relevant regulatory role appears unlikely, given ambient cell nucleotide concentrations. It is of interest to note that in V-type ATPases, nucleotide sites are present on the three B subunits [282–284]. B subunits of V-ATPases are thought to be analogous to α subunits of F_1F_0, thus these sites may correspond to the noncatalytic sites of F_1. The conservation of these sites in analogous enzymes may be indicative of the fact that a role does exist for noncatalytic sites; perhaps studies of V-ATPases will uncover it.

6. Conclusion

This review has dealt with one of the fundamental processes of biology, the mechanism by which the enzyme F_1F_0-ATP synthase carries out ATP synthesis. Numerous researchers have contributed to advance the knowledge of F_1F_0-ATP synthase to its present-day level. In computer databases more than 1000 entries on this topic can be found for the last four years alone. We apologize to everyone whose work we could not, or not adequately, discuss; we did intentionally restrict our focus to the catalytic mechanism, with emphasis on new developments, and we hope to have demonstrated that progress has been remarkable. Four advances stand out, namely: (1) knowledge of the structure of the membrane subunit *c* and the mechanism of transmembrane proton transport; (2) structure/function resolution of the stalk subunits involved in coupling, notably γ and ϵ; (3) definition of the structure of F_1 by X-ray crystallography; and (4) development of direct optical probes of nucleotide binding and hydrolysis in catalytic sites.

What are important future directions? Of course everyone has their own thoughts. Here are ours. First, it seems that one can never know enough about structure, and, perversely, the more complex an enzyme is, the more one needs to know about structure to understand mechanism. Thus, a high resolution structure of F_0 and the stalk is required. Second, there is increasing evidence concerning – and corresponding interest in – the idea that substantial subunit movements occur in the course of the catalytic cycle. Speculations about subunit rotation have been around for some time. There is a clear need for development of direct techniques to measure subunit movement on real time scale. Third, mechanistic studies in the past have usually employed the hydrolysis reaction; in the future, emphasis should be directed to analysing the properties and behavior of the three catalytic sites during steady-state ATP synthesis in the presence of a proton gradient. Fourth, at the molecular level, we can just now begin to discern how the affinity for ATP is determined by specific catalytic site ligands, and to hypothesize how changes in affinity, leading to energized release of ATP from the catalytic sites during oxidative phosphorylation, could be brought about. These ideas need to be tested and refined.

The field is as vigorous as ever. The F_1 X-ray structure has generated enhanced interest and excitement, attracting attention to F_1F_0 from researchers in many fields. For more senior investigators it has brought deep satisfaction, confirming older work, yet revealing the enzyme with clarity and sharpness hitherto unattainable. For younger investigators it surely presents opportunities to accomplish important research. With several other experimental approaches flourishing concomitantly, the future looks most promising.

Acknowledgements

Supported by NIH grant GM25349.

References

[1] Senior, A.E. (1990) Annu. Rev. Biophys. Biophys. Chem. 19, 7–41.
[2] Fillingame, R.H. (1990) in The Bacteria (T.A. Krulwich, ed.), Vol. XII, Academic Press, New York, pp. 345–391.
[3] Penefsky, H.S. and Cross, R.L. (1991) Adv. Enzymol. 64, 173–214.
[4] Cox, G.B., Devenish, R.J., Gibson, F., Howitt, S.M. and Nagley, P. (1992) in Molecular Mechanisms in Bioenergetics (L. Ernster, ed.), Elsevier, Amsterdam, pp. 283–315.

[5] Issartel, J.P., Dupuis, A., Garin, J., Lunardi, J., Michel, L. and Vignais, P.V. (1992) Experientia 48, 351–362.
[6] Hatefi, Y. (1993) Eur. J. Biochem. 218, 759–767.
[7] Pedersen, P.L. and Amzel, L.M. (1993) J. Biol. Chem. 268, 9937–9940.
[8] Capaldi, R.A., Aggeler, R., Turina, P. and Wilkens, S. (1994) Trends Biochem. Sci. 19, 284–289.
[9] Nakamoto, R.K. (1996) J. Membr. Biol. 151, 101–111.
[10] Pedersen, P.L. and Amzel, L.M. (eds.) (1992) J. Bioenerg. Biomembr. 23, 427–506.
[11] Moore, A.L. (1995) Biochem. Soc. Transac. 23, 735–793.
[11a] Boyer, P.D. (1981) in Of Oxygen, Fuels and Living Matter G. Semenza, ed.), Part I, Wiley, New York, pp. 229–264.
[12] Rao, R. and Senior, A.E. (1987) J. Biol. Chem. 262, 17450–17454.
[13] Abrahams, J.P., Leslie, A.G.W., Lutter, R. and Walker, J.E. (1994) Nature 370, 621–628.
[14] Walker, J.E., Saraste, M. and Gay, N.J. (1984) Biochim. Biophys. Acta 768, 164–200.
[15] Dunn, S.D. and Heppel, L.A. (1981) Arch. Biochem. Biophys. 210, 421–436.
[16] Schneider, E. and Altendorf, K. (1987) Microbiol. Rev. 51, 477–497.
[17] Fromme, P., Gräber, P. and Salnikow, J. (1987) FEBS Lett. 218, 27–30.
[18] Walker, J.E. and Collinson, I.R. (1994) FEBS Lett. 346, 39–43.
[19] Collinson, I.R., Runswick, M.J., Buchanan, S.K., Fearnley, I.M., Skehel, J.M., Van Raaij, M.J., Griffiths, D.E. and Walker, J.E. (1994) Biochemistry 33, 7971–7978.
[20] Lutter, R., Saraste, M., Van Walraven, H.S., Runswick, M.J., Finel, M., Deatherage, J.F. and Walker, J.E. (1993) Biochem. J. 295, 799–806.
[21] Walker, J.E., Lutter, R., Dupuis, A. and Runswick, M.J. (1991) Biochemistry 5369–5378.
[22] Hamasur, B. and Glaser, E. (1992) Eur. J. Biochem. 205, 409–416.
[23] Morikami, A., Aiso, K., Asahi, T. and Nakamura, K. (1992) J. Biol. Chem. 267, 72–76.
[24] Pedersen, P.L., Scherzmann, K. and Cintron, N. (1981) Current Topics Bioenergetics 11, 149–199.
[25] Ichikawa, N., Yoshida, Y, Hashimoto, T., Ogasawara, N., Yoshikawa, H., Imamoto, F. and Tagawa, Y. (1990) J. Biol. Chem. 265, 6274–6278.
[26] Nelson, N. (1992) Biochim. Biophys. Acta 1100, 109–124.
[27] Solomon, K.A., Hsu, D.K.W. and Brusilow, W.S.A. (1989) J. Bacteriol. 171, 3039–3045.
[28] Schneppe, B., Deckers-Hebestreit, G. and Altendorf, K. (1991) FEBS Lett. 292, 145–147.
[29] Schneppe, B., Deckers-Hebestreit, G. and Altendorf, K. (1990) J. Biol. Chem. 265, 389–395.
[30] Schneppe, B., Deckers-Hebestreit, G., McCarthy, J.E.G. and Altendorf, K. (1991) J. Biol. Chem. 266, 21090–21098.
[31] Hsu, D.K.W. and Brusilow, W.S.A. (1995) FEBS Lett. 371, 127–131.
[32] Tiedge, H. and Schäfer, G. (1989) Biochim. Biophys. Acta 977, 1–9.
[33] Bianchet, M., Ysern, X., Hullihen, J., Pedersen, P.L. and Amzel, L.M. (1991) J. Biol. Chem. 266, 21197–21201.
[34] Weber, J., Wilke-Mounts, S., Grell, E. and Senior, A.E. (1994) J. Biol. Chem. 269, 11261–11268.
[35] McCarty, R.E. and Hammes, G.G. (1987) Trends Biochem. Sci. 12, 234–237.
[36] Watts, S.D., Zhang, Y., Fillingame, R.H. and Capaldi, R.A. (1995) FEBS Lett. 368, 235–238.
[37] Gogol, E.P., Lücken, U. and Capaldi, R.A. (1987) FEBS Lett. 219, 274–278.
[38] Lücken, U., Gogol, E.P. and Capaldi, R.A. (1990) Biochemistry 29, 5339–5343.
[39] Wilkens, S., Dahlquist, F.W., McIntosh, L.P., Donaldson, L.W. and Capaldi, R.A. (1995) Nature Struct. Biol. 2, 961–967.
[40] Lötscher, H.R., deJong, C. and Capaldi, R.A. (1984) Biochemistry 23, 4134–4140.
[41] Dallmann, H.G., Flynn, T.G. and Dunn, S.D. (1992) J. Biol. Chem. 267, 18953–18960.
[42] Aggeler, R., Haughton, M. and Capaldi, R.A. (1995) J. Biol. Chem. 270, 9185–9191.
[43] Dunn, S.D. (1982) J. Biol. Chem. 257, 7354–7359.
[44] Cox, G.B., Cromer, B.A., Guss, J.M., Harvey, I., Jeffrey, P.D. and Webb, D.C. (1993) J. Mol. Biol. 229, 1159–1162.
[44a] Soteropoulos, P., Süss, K.H. and McCarty, R.E. (1992) J. Biol. Chem. 267, 10348–10354.
[45] Gogol, E.P., Johnston, E., Aggeler, R. and Capaldi, R.A. (1990) Proc. Natl. Acad. Sci. USA 87, 9585–9589.
[46] Aggeler, R., Weinreich, F. and Capaldi, R.A. (1995) Biochim. Biophys. Acta 1230, 62–68.
[47] Zhang, Y., Oldenburg, M. and Fillingame, R.H. (1994) J. Biol. Chem. 269, 10221–10224.
[48] Zhang, Y. and Fillingame, R.H. (1995) J. Biol. Chem. 270, 24609–24614.
[49] Engelbrecht, S. and Junge, W. (1990) Biochim. Biophys. Acta 1015, 379–390.
[50] Mendel-Hartvig, J. and Capaldi, R.A. (1991) Biochim. Biophys. Acta 1060, 115–124.
[51] Engelbrecht, S., Reed, J., Penin, F., Gautheron, D.C. and Junge, W. (1991) Z. Naturforsch. 46c, 759–764.
[52] Hazard, A.L. and Senior, A.E. (1994) J. Biol. Chem. 269, 418–426.
[53] Ziegler, M., Xiao, R. and Penefsky, H.S. (1994) J. Biol. Chem. 269, 4233–4239.
[54] Archinard, P., Godinot, C., Comte, J. and Gautheron, D.C. (1986) Biochemistry 25, 3397–3404.
[55] Bragg, P.D. and Hou, C. (1986) Biochim. Biophys. Acta 851, 385–394.
[56] Joshi, S. and Burrows, R. (1990) J. Biol. Chem. 265, 14518–14525.
[57] Belogrudov, G.I., Tomich, J.M. and Hatefi, Y. (1995) J. Biol. Chem. 270, 2053–2060.
[58] Maggio, M.B., Parsonage, D. and Senior, A.E. (1988) J. Biol. Chem. 263, 4619–4623.
[59] Beckers, G., Berzborn, R.J. and Strotmann, H. (1992) Biochim. Biophys. Acta 1101, 97–104.
[60] Collinson, I.R., van Raaij, M.J., Runswick, M.J., Fearnley,

I.M., Skehel, J.M., Orriss, G.L., Miroux, B. and Walker, J.E. (1994) J. Mol. Biol. 242, 408–421.
[61] Birkenhäger, R., Hoppert, M., Deckers-Hebestreit, G., Mayer, F. and Altendorf, K. (1995) Eur. J. Biochem. 230, 58–67.
[62] Hoppe, J., Brunner, J. and Jørgensen, B.B. (1984) Biochemistry 23, 5610–5616.
[63] Vik, S.B. and Dao, N.N. (1992) Biochim. Biophys. Acta 1140, 199–207.
[64] Cox, G.B., Fimmel, A.L., Gibson, F. and Hatch, L. (1986) Biochim. Biophys. Acta 849, 62–69.
[65] Fillingame, R.H. (1992) J. Bioenerg. Biomembr. 24, 485–491.
[66] Fraga, D., Hermolin, J. and Fillingame, R.H. (1994) J. Biol. Chem. 269, 2562–2567.
[67] Lewis, M.J. and Simoni, R.D. (1992) J. Biol. Chem. 267, 3482–3489.
[68] Senior, A.E. (1983) Biochim. Biophys. Acta 726, 81–95.
[69] Schneider, E. and Altendorf, K. (1984) Proc. Natl. Acad. Sci. USA 81, 7279–7283.
[70] Schneider, E. and Altendorf, K. (1985) EMBO J. 4, 515–518.
[71] Aris, J.P. and Simoni, R.D. (1983) J. Biol. Chem. 258, 14599–14609.
[72] Hermolin, J., Gallant, J. and Fillingame, R.H. (1983) J. Biol. Chem. 258, 14550–14555.
[73] Kumamoto, C. and Simoni, R.D. (1986) J. Biol. Chem. 261, 10037–10042.
[74] Walker, J.E., Saraste, M. and Gay, N.J. (1982) Nature 298, 867–869.
[75] Jans, D.A., Hatch, L., Fimmel, A.L., Gibson, F. and Cox, G.B. (1985) J. Bacteriol. 162, 420–426.
[76] Dunn, S.D. (1992) J. Biol. Chem. 267, 7630–7636.
[77] Howitt, S.M., Rodgers, A.J.W., Jeffrey, P.D. and Cox, G.B. (1996) J. Biol. Chem. 271, 7038–7042.
[78] Wilkens, S., Dunn, S.D. and Capaldi, R.A. (1994) FEBS Lett. 354, 37–40.
[79] Girvin, M.E. and Fillingame, R.H. (1993) Biochemistry 32, 12167–12177.
[80] Girvin, M.E. and Fillingame, R.H. (1994) Biochemistry 33, 665–674.
[81] Girvin, M.E. and Fillingame, R.H. (1995) Biochemistry 34, 1635–1645.
[82] Girvin, M.E., Hermolin, J., Pottorf, R. and Fillingame, R.H. (1994) Biochemistry 28, 4340–4343.
[83] Hensel, M., Deckers-Hebestreit, G., Schmid, R. and Altendorf, K. (1990) Biochim. Biophys. Acta 1016, 63–70.
[84] Schemidt, R.A., Hsu, D.K.W., Deckers-Hebestreit, G., Altendorf, K. and Brusilow, W.S.A. (1995) Arch. Biochem. Biophys. 323, 423–428.
[85] Vik, S.B. and Antonio, B.J. (1994) J. Biol. Chem. 269, 30364–30369.
[86] Böttcher, B., Gräber, P., Boekema, E.J. and Lücken, U. (1995) FEBS Lett. 373, 262–264.
[87] Duncan, T.M., Bulygin, V.V., Zhou, Y., Hutcheon, M.L. and Cross, R.L. (1995) Proc. Natl. Acad. Sci. USA 92, 10964–10968.
[88] Harris, D.A. (1995) Biochem. Soc. Transac. 23, 790–793.
[89] Penin, F., Deléage, G., Gagliardi, D., Roux, B. and Gautheron, D.C. (1990) Biochemistry 29, 9358–9364.
[90] Orriss, G.L., Runswick, M.J., Collinson, I.R., Miroux, B., Fearnley, I.M., Skehel, J.M. and Walker, J.E. (1996) Biochem. J. 314, 695–700.
[91] Hekman, C., Tomich, J.M. and Hatefi, Y. (1991) J. Biol. Chem. 266, 13564–13571.
[92] Penefsky, H.S. (1985) Proc. Natl. Acad. Sci. USA 82, 1589–1593.
[93] Matsuno-Yagi, A., Yagi, T. and Hatefi, Y., (1985) Proc. Natl. Acad. Sci. USA 82, 7550–7554.
[94] Dimroth, P. (1987) Microbiol. Rev. 51, 320–340.
[95] Laubinger, W. and Dimroth, P. (1988) Biochemistry 27, 7531–7537.
[96] Reidlinger, J. and Müller, V. (1994) Eur. J. Biochem. 223, 275–283.
[97] Forster, A., Daniel, R. and Müller, V. (1995) Biochim. Biophys. Acta 1229, 393–397.
[98] Dmitriev, O., Deckers-Hebestreit, G. and Altendorf, K. (1993) J. Biol. Chem. 268, 14776–14780.
[99] Al-Shawi, M.K. and Senior, A.E. (1992) Biochemistry 31, 878–885.
[100] Labahn, A. and Gräber, P. (1992) FEBS Lett. 313, 177–180.
[101] Gräber, P. and Labahn, A. (1992) J. Bioenerg. Biomembr. 24, 493–497.
[102] Weber, J., Wilke-Mounts, S., Lee, R.S.F., Grell., E. and Senior, A.E. (1993) J. Biol. Chem. 268, 20126–20133.
[103] Weber, J. and Senior, A.E. (1996) J. Biol. Chem. 271, 3474–3477.
[104] Gräber, P. (1994) Biochim. Biophys. Acta 1187, 171–176.
[105] Pitard, B., Richard, P., Dunach, M. and Rigaud, J. (1996) Eur. J. Biochem. 235, 779–788.
[106] Vik, S.B., Lee, D., Curtis, C.E. and Nguyen, L.T. (1990) Arch. Biochem. Biophys. 282, 125–131.
[107] Hartzog, P.E. and Cain, B.D. (1993) J. Bacteriol. 175, 1337–1343.
[108] Hartzog, P.E. and Cain, B.D. (1993) J. Biol. Chem. 269, 32313–32317.
[109] Eya, S., Maeda, M. and Futai, M. (1991) Arch. Biochem. Biophys. 284, 71–77.
[110] Paule, C.R. and Fillingame, R.H. (1989) Arch. Biochem. Biophys. 274, 270–284.
[111] Howitt, S.M. and Cox, G.B. (1992) Proc. Natl. Acad. Sci. USA 89, 9799–9803.
[112] Hatch, L.P., Cox, G.B. and Howitt, S.M. (1995) J. Biol. Chem. 270, 29407–29412.
[113] Wang, S. and Vik, S.B. (1994) J. Biol. Chem. 269, 3095–3099.
[114] Dimroth, P. (1995) Biochem. Soc. Transac. 23, 770–775.

[115] Senior, A.E. (1988) Physiol. Rev. 68, 177–231.
[116] Galanis, M., Mattoon, J.R. and Nagley, P. (1989) FEBS Lett. 249, 333–336.
[117] Hoppe, J. and Sebald, W. (1984) Biochem. Biophys. Acta 768, 1–27.
[118] Dmitriev, O.Y., Altendorf, K. and Fillingame, R.H. (1995) Eur. J. Biochem. 233, 478–483.
[119] Hermolin, J. and Fillingame, R.H. (1989) J. Biol. Chem. 264, 3896–3903.
[120] Cox, G.B., Jans, D.A., Fimmel, A.L., Gibson, F. and Hatch, L. (1984) Biochim. Biophys. Acta 768, 201–208.
[121] Fillingame, R.H., Girvin, M.E. and Zhang, Y. (1995) Biochem. Soc. Transac. 23, 760–766.
[122] Norwood, T.J., Crawford, D.A., Steventon, M.E., Driscoll, P. and Campbell, I.D. (1992) Biochemistry 31, 6285–6291.
[123] Miller, M.J., Oldenburg, M. and Fillingame, R.H. (1990) Proc. Natl. Acad. Sci. USA 87, 4900–4904.
[124] Zhang, Y. and Fillingame, R.H. (1994) J. Biol. Chem. 269, 5473–5479.
[125] Assadi-Porter, F. and Fillingame, R.H. (1995) Biochemistry 34, 16186–16193.
[126] Kluge, C. and Dimroth, P. (1993) J. Biol. Chem. 268, 14557–14560.
[127] Kluge, C. and Dimroth, P. (1993) Biochemistry 32, 10378–10386.
[128] Kluge, C. and Dimroth, P. (1995) FEBS Lett. 340, 245–248.
[129] Kluge, C. and Dimroth, P. (1992) Biochemistry 31, 12665–12672.
[130] Zhang, Y. and Fillingame, R.H. (1995) J. Biol. Chem. 270, 87–93.
[131] Kaim, G. and Dimroth, P. (1995) J. Mol. Biol. 253, 726–738.
[132] Spruth, M., Reidlinger, J. and Müller, V. (1995) 1229, 96–102.
[133] Fillingame, R.H. (1992) Biochim. Biophys. Acta 1101, 240–243.
[134] Mosher, M.E., White, L.K., Hermolin, J. and Fillingame, R.H. (1985) J. Biol. Chem. 260, 4807–4814.
[135] Fraga, D. and Fillingame, R.H. (1989) J. Biol. Chem. 264, 6797–6803.
[136] Miller, M.J., Fraga, D., Paule, C.R. and Fillingame, R.H. (1989) J. Biol. Chem. 264, 305–311.
[137] Fraga, D., Hermolin, J., Oldenburg, M., Miller, M.J. and Fillingame, R.H. (1994) J. Biol. Chem. 269, 7532–7537.
[138] Jounouchi, M., Takeyama, M., Chaiprasert P., Noumi, T., Moriyama, Y., Maeda, M. and Futai, M. (1992) Arch. Biochem. Biophys. 292, 376–381.
[139] Joshi, S., Javed, A.A. and Gibbs, L.C. (1992) J. Biol. Chem. 267, 12860–12867.
[140] Hazard, A.L. and Senior, A.E. (1994) J. Biol. Chem. 269, 427–432.
[141] Aggeler, R. and Capaldi, R.A. (1996) J. Biol. Chem. 271, 13888–13891.
[142] Haughton, M.A. and Capaldi, R.A. (1995) J. Biol. Chem. 270, 20568–20574.
[143] Wilkens, S. and Capaldi, R.A. (1994) Biol. Chem. Hoppe-Seyler 375, 43–51.
[144] Capaldi, R.A., Aggeler, R. and Wilkens, S. (1995) Biochem. Soc. Transac. 23, 767–770.
[145] Shin, K., Nakamoto, R.K., Maeda, M. and Futai, M. (1992) J. Biol. Chem. 267, 20835–20839.
[146] Nakamoto, R.K., Maeda, M. and Futai, M. (1993) J. Biol. Chem. 268, 867–872.
[147] Nakamoto, R.K., Al-Shawi, M.K. and Futai, M. (1995) J. Biol. Chem. 270, 14042–14046.
[148] Jeanteur-De Beukelaer, C.J., Omote, H., Iwamoto-Kihara, A., Maeda, M. and Futai, M. (1995) J. Biol. Chem. 270, 22850–22854.
[149] Aggeler, R. and Capaldi, R.A. (1992) J. Biol. Chem. 267, 21355–21358.
[150] Aggeler, R. and Capaldi, R.A. (1993) J. Biol. Chem. 268, 14576–14579.
[151] Aggeler, R., Cai, S.X., Keana, J.F.W., Koike, T. and Capaldi, R.A. (1993) J. Biol. Chem. 268, 20831–20837.
[152] Turina, P. and Capaldi, R.A. (1994) J. Biol. Chem. 269, 13465–13471.
[153] Turina, P. and Capaldi, R.A. (1994) Biochemistry 33, 14275–14280.
[154] Tang, C. and Capaldi, R.A. (1996) J. Biol. Chem. 271, 3018–3024.
[155] Skakoon, E.N. and Dunn, S.D. (1993) Arch. Biochem. Biophys. 302, 272–278.
[156] Grüber, G. and Capaldi, R.A. (1996) Biochemistry 35, 3875–3879.
[157] Penefsky, H.S. (1985) J. Biol. Chem. 260, 13735–13741.
[158] Xiao, R. and Penefsky, H.S. (1994) J. Biol. Chem. 269, 19232–19237.
[159] Souid, A.K. and Penefsky, H.S. (1994) J. Bioenerg. Biomembr. 26, 627–630.
[160] Souid, A.K. and Penefsky, H.S. (1995) J. Biol. Chem. 270, 9074–9082.
[161] Kashket, E.R. (1982) Biochemistry 21, 5534–5538.
[162] Weber, J. and Senior, A.E. (1995) J. Biol. Chem. 270, 12653–12658.
[163] Al-Shawi, M.K., Parsonage, D. and Senior, A.E. (1990) J. Biol. Chem. 265, 4402–4410.
[164] Fischer, S., Etzold, C., Turina, P., Deckers-Hebestreit, G., Altendorf, K. and Gräber, P. (1994) Eur. J. Biochem. 225, 167–172.
[165] Penefsky, H.S. (1985) J. Biol. Chem. 260, 13728–13734.
[166] Zhou, Y., Duncan, T.M., Bulygin, V.V., Hutcheon, M.L. and Cross, R.L. (1996) Biochim. Biophys. Acta 1275, 96–100.
[167] Walker, J.E., Saraste, M., Runswick, M.J. and Gay, N.J. (1982) EMBO J. 1, 945–951.
[168] Rao, R., Pagan, J. and Senior, A.E. (1988) J. Biol. Chem. 263, 15957–15963.
[169] Senior, A.E. and Al-Shawi, M.K. (1992) J. Biol. Chem. 267, 21471–21478.
[170] Weber, J., Bowman, C., Wilke-Mounts, S. and Senior, A.E. (1995) J. Biol. Chem. 270, 21045–21049.

[171] Ohta, S., Tsuboi, M., Oshima, T., Yoshida, M. and Kagawa, Y. (1980) J. Biochem. 87, 1609–1617.
[172] Issartel, J.P. and Vignais, P.V. (1984) Biochemistry 23, 6591–6595.
[173] Rao, R., Al-Shawi, M.K. and Senior, A.E. (1988) J. Biol. Chem. 263, 5569–5573.
[174] Mills, D.A. and Richter, M.L. (1991) J. Biol. Chem. 266, 7440–7444.
[175] Al-Shawi, M.K., Parsonage, D. and Senior, A.E. (1990) J. Biol. Chem. 265, 5595–5601.
[176] Dunn, S.D. and Futai, M. (1980) J. Biol. Chem. 255, 113–118.
[177] Noumi, T., Maeda, M. and Futai, M. (1988) J. Biol. Chem. 263, 8765–8770.
[178] Gao, F., Lipscomb, B., Wu, I. and Richter, M.L. (1995) J. Biol. Chem. 270, 9763–9769.
[179] Kagawa, Y., Ohta, S. and Otawara-Hamamoto, Y. (1989) FEBS Lett. 249, 67–69.
[180] Miwa, K. and Yoshida, M. (1989) Proc. Natl. Acad. Sci. USA 86, 6484–6487.
[181] Ohta, S., Harada, M., Ito, Y., Kobayashi, Y., Sone, N. and Kagawa, Y. (1990) Biochem. Biophys. Res. Commun. 171, 1258–1263.
[182] Saika, K. and Yoshida, M. (1995) FEBS Lett. 368, 207–210.
[183] Kaibara, C., Matsui, T., Hisabori, T. and Yoshida, M. (1996) J. Biol. Chem. 271, 2433–2438.
[184] Lutter, R., Abrahams, J.P., Van Raaij, M.J., Lundqvist, T., Buchanan, S.K., Leslie, A.G.W. and Walker, J.E. (1993) J. Mol. Biol. 229, 787–790.
[185] Cross, R.L. (1994) Nature 370, 594–595.
[186] Cross, R.L., Grubmeyer, C. and Penefsky, H.S. (1982) J. Biol. Chem. 257, 12101–12105.
[187] Al-Shawi, M.K., Parsonage, D. and Senior, A.E. (1988) J. Biol. Chem. 263, 19633–19639.
[188] Junesch, U. and Gräber, P. (1987) Biochim. Biophys. Acta 893, 275–288.
[189] Matsuno-Yagi, A. and Hatefi, Y. (1988) Biochemistry 27, 335–340.
[190] Penefsky, H.S. (1986) Methods Enzymol. 126, 608–618.
[191] Duncan, T.M. and Senior, A.E. (1985) J. Biol. Chem. 260, 4901–4907.
[192] Senior, A.E. (1992) J. Bioenerg. Biomembr. 24, 479–484.
[193] Wise, J.G., Latchney, L.R., Ferguson, A.M. and Senior, A.E. (1984) Biochemistry 23, 1426–1432.
[194] Harris, D.A. (1989) Biochim. Biophys. Acta 974, 156–162.
[195] Noumi, T., Maeda, M. and Futai, M. (1987) FEBS Lett. 213.
[196] Senior, A.E., Lee, R.S.F., Al-Shawi, M.K. and Weber, J. (1992) Arch. Biochem. Biophys. 297, 340–344.
[197] Dunn, S.D., Zadorozny, V.D., Tozer, R.G. and Orr, L.E. (1987) Biochemistry 26, 4488–4493.
[198] Roisin, M.P. and Kepes, A. (1972) Biochim. Biophys. Acta 275, 333–346.
[199] Kobayashi, H. and Anraku, Y. (1972) J. Biochem. 71, 387–399.
[200] Boyer, P.D. (1993) Biochim. Biophys. Acta 1140, 215–250.
[201] Fersht, A.R. (1985) Enzyme Structure and Mechanism, 2nd edn., W.H. Freeman, New York, p. 236.
[202] Webb, M.R., Grubmeyer, C., Penefsky, H.S. and Trentham, D.R. (1980) J. Biol. Chem. 255, 11637–11639.
[203] Senter, P., Eckstein, F. and Kagawa, Y. (1983) Biochemistry 22, 5514–5518.
[204] Issartel, J.P., Dupuis, A., Lunardi, J. and Vignais, P.V. (1991) Biochemistry 30, 4726–4733.
[205] Fisher, A.J., Smith, C.A., Thoden, J.B., Smith, R., Sutoh, K., Holden, H.M. and Rayment, I. (1995) Biochemistry 34, 8960–8972.
[206] Sondek, J., Lambright, D.G., Noel, J.P., Hamm, H.E. and Sigler, P.B. (1994) Nature 372, 276–279.
[207] Mueller, D.M. (1989) J. Biol. Chem. 264, 16552–16556.
[208] Park, M.Y., Omote, H., Maeda, M. and Futai, M. (1994) J. Biochem. 116, 1139–1145.
[209] Al-Shawi, M.K. and Senior, A.E. (1992) Biochemistry 31, 886–891.
[210] Boyer, P.D. (1989) FASEB J. 3, 2164–2178.
[211] O'Neal, C.C. and Boyer, P.D. (1984) J. Biol. Chem. 259, 5761–5767.
[212] Wood, J.M., Wise, J.G., Senior, A.E., Futai, M. and Boyer, P.D. (1987) J. Biol. Chem. 262, 2180–2186.
[213] Allison, W.S., Jault, J.M., Grodsky, N.B. and Dou, C. (1995) Biochem. Soc. Transac. 23, 752–756.
[214] Cross, R.L. (1981) Annu. Rev. Biochem. 50, 681–714.
[215] Cross, R.L. (1992) in Molecular Mechanisms in Bioenergetics (Ernster, L., ed.), pp. 317–330, Elsevier, Amsterdam.
[216] Gresser, M.J., Myers, J.A. and Boyer, P.D. (1982) J. Biol. Chem. 257, 12030–12038.
[217] Adolfsen, R. and Moudrianakis, E.N. (1976) Arch. Biochem. Biophys. 172, 425–433.
[218] Kayalar, C., Rosing, J. and Boyer, P.D. (1977) J. Biol. Chem. 252, 2486–2491.
[219] Boyer, P.D. (1979) In Membrane Bioenergetics (Lee, C.P., Schatz, G. and Ernster, L., eds.), pp. 461–479, Addison-Wesley, Reading, MA.
[220] Weber, J., Wilke-Mounts, S. and Senior, A.E. (1994) J. Biol. Chem. 269, 20462–20467.
[221] Hirano, M., Takeda, K., Kanazawa, H. and Futai, M. (1984) Biochemistry 23, 1652–1656.
[222] Senior, A.E., Wilke-Mounts, S. and Al-Shawi, M.K. (1993) J. Biol. Chem. 268, 6989–6994.
[223] Weber, J., Bowman, C. and Senior, A.E. (1996) J. Biol. Chem. 271, 18711–18718.
[224] Wilke-Mounts, S., Weber, J., Grell, E. and Senior, A.E. (1994) Arch. Biochem. Biophys. 309, 363–368.
[225] Garin, J., Boulay, F., Issartel, J.P., Lunardi, J. and Vignais, P.V. (1986) Biochemistry 25, 4431–4437.
[226] Cross, R.L., Cunningham, D., Miller, C.G., Xue, Z., Zhou, J.M. and Boyer P.D. (1987) Proc. Natl. Acad. Sci. USA 84, 5715–5719.
[227] Wise, J.G., Hicke, B.J. and Boyer, P.D. (1987) FEBS Lett. 223, 395–401.
[228] Admon, A. and Hammes, G.G. (1987) Biochemistry 26, 3193–3197.

[229] Bullough, D.A. and Allison, W.S. (1986) J. Biol. Chem. 261, 14171–14177.
[230] Xue, Z., Miller, C.G., Zhou, J.M. and Boyer, P.D. (1987) FEBS Lett. 223, 391–394.
[231] Garin, J., Vinçon, M., Gagnon, J. and Vignais, P.V. (1994) Biochemistry 33, 3772–3777.
[232] Weber, J., Lee, R.S.F., Grell, E., Wise, J.G. and Senior, A.E. (1992) J. Biol. Chem. 267, 1712–1718.
[233] Wise, J.G. (1990) J. Biol. Chem. 265, 10403–10409.
[234] Odaka, K., Kaibara, C., Amano, T., Matsui, T., Muneyuki, E., Ogasahara, K., Yutani, K. and Yoshida, M. (1994) J. Biochemistry 115, 789–796.
[235] Pai, E., Kabsch, W., Krengel, U., Holmes, K.C., John, J. and Wittinghofer, A. (1989) Nature 341, 209–214.
[236] Müller, C.W. and Schulz, G.E. (1992) J. Mol. Biol. 224, 159–177.
[237] Story, R.M. and Steitz, T.A. (1992) Nature 355, 374–376.
[238] Jurnak, F. (1985) Science 230,32–36.
[239] Berchtold, H., Reshetnikova, L., Reiser, C.O., Schirmer, N.K., Sprinzl, M. and Hilgenfeld, R. (1993) Nature 365, 126–132.
[240] Iwamoto, A., Omote, H., Hanada, H., Tomioka, N., Itai, A., Maeda, M. and Futai, M. (1991) J. Biol. Chem. 266, 16350–16355.
[241] Iwamoto, A., Park, M.Y., Maeda, M. and Futai, M. (1993) J. Biol. Chem. 268, 3156–3160.
[242] Shen, H., Yao, B. and Mueller, D.M. (1994) J. Biol. Chem. 269, 9424–9428.
[243] Mueller, D.M. (1989) Biochem. Biophys. Res. Commun. 164, 381–386.
[244] Yohda, M., Ohta, S., Hisabori, T. and Kagawa, Y. (1988) Biochim. Biophys. Acta 933, 156–164.
[245] Omote, H., Maeda, M. and Futai, M. (1992) J. Biol. Chem. 267, 20571–20576.
[246] Omote, H., Le, N.P., Park, M.Y., Maeda, M. and Futai, M. (1995) J. Biol. Chem. 270, 25656–25660.
[247] Amano, T., Tozawa, K., Yoshida, M. and Murakami, H. (1994) FEBS Lett. 348, 93–99.
[248] Al-Shawi, M.K., Parsonage, D. and Senior, A.E. (1989) J. Biol. Chem. 264, 15376–15383.
[249] Wilke-Mounts, S., Pagan, J. and Senior, A.E. (1995) Arch. Biochem. Biophys. 324, 153–158.
[250] Noumi, T., Taniai, M., Kanazawa, H. and Futai, M. (1986) J. Biol. Chem. 261, 9196–9201.
[251] Soga, S., Noumi, T., Takeyama, M., Maeda, M. and Futai, M. (1989) Arch. Biochem. Biophys. 268, 643–648.
[252] Turina, P., Aggeler, R., Lee, R.S.F., Senior, A.E. and Capaldi, R.A. (1993) J. Biol. Chem. 268, 6978–6984.
[253] Noumi, T., Futai, M. and Kanazawa, H. (1984) J. Biol. Chem. 259, 10076–10079.
[254] Maggio, M.B., Pagan, J., Parsonage, D., Hatch, L. and Senior, A.E. (1987) J. Biol. Chem. 262, 8981–8984.
[255] Wise, J.G., Latchney, L.R. and Senior, A.E. (1981) J. Biol. Chem. 256, 10383–10389.
[256] Lee, R.S.F., Wilke-Mounts, S. and Senior, A.E. (1992) Arch. Biochem. Biophys. 297, 334–339.
[257] Houseman, A.L.P., LoBrutto, R., Frasch, W.D. (1995) Biochemistry 34, 3277–3285.
[258] Pai, E.F., Krengel, U., Petsko, G.A., Goody, R.S., Kabsch, W. and Wittinghofer, A. (1990) EMBO J. 9, 2351–2359.
[259] Goody, R.S., Pai, E.F., Schlichting, I., Rensland, H., Scheidig, A., Franken, S. and Wittinghofer, A. (1992) Phil. Trans. R. Soc. Lond. B 336, 3–11.
[260] Chung, H.H., Benson, D.R. and Schultz, P.G. (1993) Science 259, 806–809.
[261] Langen, R., Schweins, T. and Warshel, A. (1992) Biochemistry 31, 8691–8696.
[262] Schweins, T., Langen, R. and Warshel, A. (1994) Nature Struct. Biol. 1, 476–484.
[263] Schweins, T., Geyer, M., Scheffzek, K., Warshel, A., Kalbitzer, H.R. and Wittinghofer, A. (1995) Nature Struct. Biol. 2, 36–44.
[264] Coleman, D.E., Berghuis, A.M., Lee, E., Linder, E.L., Gilman, A.G. and Sprang, S.R. (1994) Science 265, 1405–1412.
[265] Webb, M.R. and Trentham, D.R. (1981) J. Biol. Chem. 256, 10910–10916.
[266] Dunn, S.D. (1980) J. Biol. Chem. 255, 11857–11860.
[267] Rao, R., Cunningham, D., Cross, R.L. and Senior, A.E. (1988) J. Biol. Chem. 263, 5640–5645.
[268] Wise, J.G., Duncan, T.M., Latchney, L.R., Cox, D.N. and Senior, A.E. (1983) Biochem. J. 215, 343–350.
[269] Cross, R.L. and Nalin, C.M. (1982) J. Biol. Chem. 257, 2874–2881.
[270] Harris D.A. (1978) Biochim. Biophys. Acta 463, 245–273.
[271] Pagan, J. and Senior, A.E. (1990) FEBS Lett. 273, 147–149.
[272] Matsui, T., Jault, J.M., Allison, W.S. and Yoshida, M. (1996) Biochem. Biophys. Res. Commun. 220,94–97.
[273] Weber, J., Lee, R.S.F., Wilke-Mounts, S., Grell, E. and Senior, A.E. (1993) J. Biol. Chem. 268, 6241–6247.
[274] Allison, W.S., Jault, J.M., Zhuo, S. and Paik, S.R. (1992) J. Bioenerg. Biomembr. 24, 469–477.
[275] Perlin D.S., Latchney L.R., Wise J.G. and Senior, A.E. (1984) Biochemistry 23, 4998–5003.
[276] Milgrom, Y.M. and Cross, R.L. (1993) J. Biol. Chem. 268, 23179–23185.
[277] Jault, J.M. and Allison, W.S. (1993) J. Biol. Chem. 268, 1558–1566.
[278] Hyndman, D.J., Milgrom, Y.M., Bramhall, E.A. and Cross, R.L. (1994) J. Biol. Chem. 269, 28871–28877.
[279] Jault, J.M., Paik, S.R., Grodsky, N.B. and Allison, W.S. (1994) Biochemistry 33, 14979–14985.
[280] Wise, J.G. and Senior A.E. (1985) Biochemistry 24, 6949–6954.
[281] Richard, P., Pitard, B. and Rigaud, J. (1995) J. Biol. Chem. 270, 21571–21578.
[282] Manolson, M.F., Rea, P.A. and Poole, R.J. (1985) J. Biol. Chem. 260, 12273–12279.
[283] Zhang, J., Vasilyeva, E., Feng, Y. and Forgac, M. (1995) J. Biol. Chem. 270, 15494–15500.
[284] Peng, S. (1995) J. Biol. Chem. 270, 16926–16931.